

Modelling uranium leaching kinetics

A thesis submitted in partial fulfilment of the requirements for the degree of

M.Sc. in (Applied Sciences) (Metallurgy)

Bernard Sililo

DEPARTMENT OF MATERIALS SCIENCE AND
METALLURGICAL ENGINEERING

FACULTY OF ENGINEERING, BUILT ENVIRONMENT AND
INFORMATION TECHNOLOGY

UNIVERSITY OF PRETORIA

PRETORIA

November 2016

Modelling of uranium leach kinetics

Bernard Liswani Sililo

Supervisor: Dr. Dick Groot

Department: Materials Science and Metallurgical Engineering

Faculty: Engineering, Built Environment and Information Technology

Degree: Masters in Applied Science: Metallurgy

ABSTRACT

The uranium price decline has negatively impacted on the uranium mining industry. This decline in price requires that uranium metallurgical processes be made to operate more efficiently. Some key parameters that influence the dissolution and kinetics of leaching uraninite (one of the main minerals from which uranium can be extracted) are pH, oxidation-reduction potential and iron concentration. A good understanding of the effect these parameters have on the leach kinetics would lead to an efficient operation of metallurgical processes. The objective of this work was therefore to investigate the effects of these key drivers on leach kinetics of Rössing Uranium ore. Added to this, was an attempt to come up with a mathematical model which can successfully replicate the leach kinetics. A series of laboratory leach experiments were performed on Rössing ore where the pH, oxidation-reduction potential and total iron were varied, one at a time, to establish the effects they have on the leach kinetics and on the uranium extraction.

Analysis of the data collected from this study showed that the leach kinetics are more dependent on the oxidation-reduction potential, followed by the iron concentration and least affected by the pH. It was further shown that oxidation-reduction potential is a function of total iron. An integral method was used to analyse the kinetic data. A literature study reveals that uraninite dissolution follows first order kinetics, but of interest in these results was that the uranium dissolution was found to closely follow the second order. Further research is recommended to look at ascertaining these results. Two models were developed, one

using regression and the other by curve fitting method. Both models could fit the experimental data well enough.

Key words: Uraninite, leach kinetics, oxidation-reduction potential, integral method

Acknowledgements

First and above all, I would like to acknowledge God for all the blessings he has bestowed on me in terms of resources and people, some of whom are the reason this work was possible. I would therefore like to offer my thanks to all of them.

Dr Dick Groot, my thanks for accepting me as your student. Your belief in me is one thing that kept me going. Added to this, thank you for your patient guidance, encouragement and the advice you provided throughout my time as your student. I would also like to thank Rössing Uranium Ltd.'s Processing department, especially the Improvement team, for allowing me to use their laboratories.

I wish to express my gratitude to my wife, Juliet, and our two sons Joshua and Jordan for their continued support, encouragement and understanding. I was continually amazed by her belief in me even when things seemed not to go my way during my research.

Finally, I would like to thank my colleagues in the department of Mining and Process Engineering at the Namibia University of Science and Technology; I forever remain indebted to you for proof reading my work and giving me some suggestions.

Dedication

To my wife Juliet and our two sons Joshua and Jordan

&

The lovely memory of my beloved parents Sililo and Chuma

Undertaking

I certify that the research work titled “*Modeling uranium leach kinetics*” is my own work. The work has not been presented elsewhere for assessment. Where material has been used from other sources, it has been properly acknowledged / referred.



Table of contents

Acknowledgements	iii
Dedication.....	iv
Undertaking	v
Table of contents	vi
List of tables.....	x
Chapter 1: Introduction	- 1 -
Chapter 2: Literature review	- 4 -
2.1 Mineralogy of Rössing Uranium Ore	- 4 -
2.2 Chemistry of uranium leaching	- 5 -
2.2.1 Proposed mechanisms of uranium dissolution	- 8 -
2.2.2 Oxidants	- 14 -
2.3 Operating parameters of interest.....	- 15 -
2.3.1 Pulp density	- 16 -
2.3.2 Iron concentration	- 17 -
2.3.3 Oxidation/reduction potential	- 21 -
2.3.4 Effects of pH	- 22 -
2.3.5 Effect of temperature on the reaction rate.....	- 25 -
2.4 Modelling of the leach kinetics	- 26 -
2.5 Conclusions and research direction	- 33 -
Chapter 3: Leaching method verification	- 35 -
3.1 Background	- 35 -
3.2 Method	- 35 -
3.3 Results and discussion	- 38 -
3.3.1 Analytical error.....	- 38 -
3.3.2 Sub-sampling error.....	- 39 -
3.3.3 Overall test error	- 39 -
3.4 Conclusion and recommendations	- 41 -
Chapter 4: Materials and methods	- 43 -
4.1 Bulk sample collection and blending	- 43 -
4.2 Reagents	- 44 -
4.3 Iron dissolution tests	- 45 -
4.4 The two-leach method.....	- 46 -
Chapter 5: Results and Discussion.....	- 48 -



5.1	The effects of parameters on uranium extraction	- 49 -
5.1.1	The effect of total Fe concentration on uranium extraction.....	- 49 -
5.1.2	The effect of ORP on uranium extraction.....	- 51 -
5.1.3	The effect of pH on uranium extraction	- 52 -
5.2	The effect of parameters on the kinetics.....	- 52 -
5.2.1	The effect of Oxidation-Reduction Potential on leach kinetics.....	- 54 -
5.2.2	Effect of Fe(III) ion on leach kinetics	- 58 -
5.2.3	The effect of pH on Uranium dissolution rate.....	- 61 -
5.3	Full factorial design.....	- 62 -
5.3.1	The main effect that affect uranium leach kinetics	- 63 -
5.3.2	Effect of factors' interaction on uranium leach kinetics.....	- 65 -
5.4	Leach kinetics model equations	- 67 -
5.4.1	Multiple regression model.....	- 68 -
5.4.2	Exponential empirical model.....	- 68 -
5.4.3	Evaluation of the kinetic models	- 69 -
Chapter 6: Conclusion and Recommendations		- 72 -
6.1	Conclusion.....	- 72 -
6.2	Recommendations	- 72 -
References.....		- 73 -
Appendix A		- 78 -
Appendix B		- 80 -
Bulk Control Sample Preparation		- 80 -
Appendix C		- 81 -
Preparation of residue sample for analysis		- 81 -
Appendix D		- 82 -
Determination of ferric/ferrous in plant solutions.....		- 82 -
Appendix E.....		- 83 -
Uranium containing minerals.....		- 83 -
Appendix F.....		- 84 -

List of figures

Figure 2. 1: Eh/pH diagram of U-S-H ₂ O system at 25 ⁰ C. Source: (Hayes, 2003)	- 7 -
Figure 2. 2: Experimentally determined relationship between Fe(III)/Fe(II) ratio and ORP of Rössing plant solutions (3M Ag/AgCl electrode).....	- 10 -
Figure 2. 3: Schematic representation of processes occurring during oxidative dissolution of UO ₂ in a geological Vault. Source: (Sunder and Shoesmith, 1991)....	- 11 -
Figure 2. 4: Effect of pulp density on uranium leaching. Source: (Tamrakar <i>et al.</i> , 2010)	- 17 -
Figure 2. 5: Plot of UO ₂ dissolution Rate versus [Fe(III)] at constant [Fe(II)] (5.04E10 ⁻³ M). Source: (Ram <i>et al.</i> , 2011)	- 18 -
Figure 2. 6: UO ₂ dissolution rate vs. total Fe for solutions at an ORP of 460 mV. Source: (Ram <i>et al.</i> , 2011)	- 19 -
Figure 2. 7: Order of UO ₂ dissolution with respect to Fe vs. solution ORP Ag/AgCl electrode. Source: (Ram <i>et al.</i> , 2011).	- 20 -
Figure 2. 8: The effect of Fe(III) concentration on the leaching rate of brannerite ore. [H ₂ SO ₄] initial = 0.5 M; temperature: 70 ⁰ C; rotation stirrer speed: 500 rpm. Source: (Gogoleva, 2012).	- 21 -
Figure 2. 9: Equilibrium iron species existing in a solution containing 0.1MFe ³⁺ and 0.5M total sulfate at 25 °C. Source: Bhappu <i>et al.</i> , (1969).	- 23 -
Figure 2. 10: The amount of uranium dissolved (%) from ore as a function of time at various H ₂ SO ₄ concentrations, M: 0.1 (1), 0.2 (2), 0.5 (3), 1.0 (4), 2.0 (5). Temperature: 70 ⁰ C; M; [Fe (III)] initial = 0.01 M, particle size: 53–74 μm. Source: (Gogoleva, 2012) -	- 24 -
Figure 2. 11: The effect of H ₂ SO ₄ concentration on the leaching rate of brannerite ore. Temperature: 70 ⁰ C; rotation stirrer speed: 500 rpm. Source: (Gogoleva, 2012).....	- 24 -
Figure 2. 12: Effect of temperature on uranium extraction. Source: (Tamrakar <i>et al.</i> , 2010).....	- 25 -
Figure 2. 13: Plots of 1 + 2(1 - a) - 3(1 - a) ^{2/3} versus time for uranium dissolution at various temperatures, °C: 35 (1), 50 (2), 60 (3), 70 (4), 80 (5), 90 (6) source: (Gogoleva, 2012).....	- 30 -
Figure 3. 1: Shows the leach reactor and baffles in leach reactor	- 37 -
Figure 3. 2: The Impeller used for stirring in the reactor	- 37 -
Figure 3. 3: The sampling device used to sub-sample from the vessel during leaching	- 38 -
Figure 3. 4: Overall extraction error at each sample time	- 40 -

Figure 3. 5: Contributions to the overall error - 41 -

**Figure 4.1: MLA particle images of uraninite (circled and in black) in the bulk control.
Source: (Ryan, 2011) - 44 -**

Figure 4. 2: The experimental set-up showing the leach vessels in the water bath. - 46 -

Figure 4. 3: The ORP probe and the probe guard - 47 -

Figure 5. 1: The effect of iron concentration of uranium extraction - 50 -

Figure 5. 2: The effect of ORP on uranium extraction - 51 -

Figure 5. 3: The effect of pH on uranium extraction - 52 -

Figure 5. 4: Test for an n^{th} -order rate form by the differential method. - 54 -

Figure 5. 5: Plot of $1/[U]$ vs. Time for the tested ORP - 55 -

Figure 5. 6: The effect of ORP on dissolution rate of Rössing Uranium ore - 56 -

Figure 5. 7: Comparison between modeled and measured ORP - 57 -

Figure 5. 8: The effect of total iron on the uranium dissolution rate at 525 mV - 58 -

Figure 5. 9: Effect of total iron on the dissolution rate - 59 -

**Figure 5. 10: The extraction achieved after 13 hours of leaching at different ORP
values - 60 -**

Figure 5. 11: The effect pH has on uranium dissolution rate - 61 -

Figure 5. 12: Pareto showing the dominant factors - 64 -

**Figure 5. 13: Plots of the main effects; a) the effect of ORP on uranium leach kinetics,
b) the effect of Fe on uranium leach kinetics, and c) the effect of pH concentration on
uranium leach kinetics. - 65 -**

Figure 5. 14: The interaction between ORP and pH - 66 -

Figure 5. 15: The interaction between ORP and $[Fe]$ - 66 -

Figure 5. 16: The interaction between total Fe and pH - 67 -

**Figure 5. 17: Comparison between the multiple regression model and experimental
data - 69 -**

Figure 5. 18: The model interface - 70 -

**Figure 5. 19: Comparison between the exponential empirical model and experimental
data - 70 -**

List of tables

Table 2. 1: Summary of previous research on Uranium dissolution rates.....	- 34 -
Table 3. 1: Conditions used in the verification leach	- 36 -
Table 4. 1: Bulk sample characterisation	- 43 -
Table 4. 2: Typical composition of recycled process solution.....	- 45 -
Table 4. 3: Dissolution test results.....	- 45 -
Table 5. 1: Shows the tests conducted to generate the kinetic data	- 48 -
Table 5. 2: Conditions kept constant throughout the test work.....	- 49 -
Table 5. 3: Shows the measured proportion of Fe(III)/Fe(II) from the Fe concentration of 0.068 M at different ORP values	- 50 -
Table 5. 4: Kinetic data used to evaluate the derivative.....	- 53 -
Table 5. 5: The rate constant k with ORP	- 56 -
Table 5. 6: Rate constant obtained from the second order integrated rate law for different iron concentration at the same ORP	- 59 -
Table 5. 7: Fe (III) concentration at 525 mV for different total iron.....	- 60 -
Table 5. 8: List of the process parameters and their levels.....	- 62 -
Table 5. 9: Coded design matrix for the three parameters and the response.....	- 63 -

Glossary of terms and abbreviations

CGS	Cordierite Gneiss Schist
CI	Calc Index: the measure of acid consuming properties of the ore
ICP – MS	Inductively Coupled Plasma Mass Spectrometry
M	Molarity, mol.dm ⁻³
MLA	Mineral Liberation Analyser
ORP	Oxidation - Reduction Potential
PCM	Progressive Conversion Model
ppm	Parts per million
ROM	Run of Mine
RSD	Relative Standard Deviation
SCE	Silver/silver-chloride electrode
SCM	Shrinking - Core Model
Standard error	A measure of the statistical accuracy of an estimate, equal to the standard deviation of the theoretical distribution of a large population of such estimates.
Uranophane	A rare mineral that forms from the oxidation of uranium-bearing minerals
Uraninite	A black, grey, or brown mineral which consists mainly of uranium dioxide and is the chief ore of uranium

Chapter 1: Introduction

1.1 Background

Uranium is the source of nuclear power from which electricity can be generated. Nuclear power is expected to be an important part of the worldwide energy mix, at least for the next 50 years, and by most projections even well beyond that period. That is, of course, provided that an adequate supply of uranium is available to sustain the nominal growth rate of nuclear power usage of 1 to 3% per year, that is as projected by some analysts (IAEA, 2001).

The World Energy Council (2013) reports that the demand for uranium is expected to continue to rise for the foreseeable future despite the Fukushima Daiichi accident. The World Energy Council (2013) further reports that nuclear power remains a significant part of the global energy mix, accounting for more than 13% of global electricity production.

In recent years, the price of uranium has dropped and this has negatively impacted many uranium mining operations. The challenges brought about by the price drop are further exacerbated by the fact that many operating mines are mining and processing low grade ores. The Fukushima incident may have had a negative impact on the uranium industry which could be contributing to the current price drop. This has become a challenge for survival in many uranium producing operations and a deterrent to the upcoming projects.

One of the ways to stay afloat during this difficult time of low grade and low prices is to produce uranium efficiently. Operating efficiently requires a deeper understanding of the process and its key drivers. In uranium leaching, some of the key drivers are pH, pulp density, oxidation-reduction potential, total iron concentration, temperature, particle size distribution and retention time, as discussed by Lunt *et al.* (2007). Oxidation–reduction potential, total iron and pH are some of the parameters that are easy to change in uraninite leaching. It is important therefore to understand how these different key drivers interact to bring about the finished product efficiently. Temperature for instance, will increase the leaching kinetics of uranium but it might not be cost effective to operate at high temperatures due to the high cost of energy. The same can be said about all the other key drivers. Therefore, there is a need to optimise the leach process.

The economic viability of many industrial processes is largely affected by the rate at which the products can be formed and the mining industry is no exception. Therefore it is vital to understand the kinetics of chemical reactions. Leaching is a central unit operation in the

hydrometallurgical treatment of ores and for this reason, much attention is focused on the study of the kinetics of leaching reactions (Crundwell, 1995). The benefit of understanding the leach kinetics is that the resources can be targeted to specific key drivers that will result in an optimised process. Crundwell (1995) proposes that in order to determine the parameters that are important in the efficient design of the hydrometallurgical plant, reliable models of both the reaction kinetics and the leaching reactor are required. The same can be said for the processing operation.

1.2 The objective of the study

The objective of this study was to better understand the leaching kinetics of Rössing Uranium ores and to be able to model the kinetics. This was achieved by studying the influence that parameters such as oxidation-reduction potential (ORP), iron concentration and pH have on leaching kinetics of the Rössing Uranium ore. The resulting model could be used to optimise the leaching process and it is a tool upon which decisions pertaining to running the process efficiently could be made.

1.3 The outline of the dissertation

The following chapters are presented in this dissertation

Chapter 1: Introduction

In this chapter, the research topic is introduced.

Chapter 2: Literature review

This chapter looks at work done on uranium leaching. This includes:

- the review on the mineralogy of Rössing Uranium ore
- the chemistry of leaching uranium and the factors that drive the kinetics of the dissolution reactions
- the current models that are used to describe the dissolution kinetics of uranium leaching.

Chapter 3: Leaching method verification

This chapter covers the work done to establish and verify the leach procedure used in the test work.

Chapter 4: Methodology

The method employed to collect data and the instruments used are discussed in this chapter.

Chapter 5: Results and Discussion

The results obtained from the test work are presented and discussed here. Conclusions and recommendations pertaining to the findings are made in this chapter.

Chapter 6: Conclusion and Recommendations

The research findings are summarised and recommendations given for future research are presented in this chapter.

Chapter 2: Literature review

This chapter looks at previous work and knowledge on the leaching of uranium. This review will be based on leaching uranium in an acidic medium; therefore the chapter will contain only a few references to alkaline leaching.

2.1 Mineralogy of Rössing Uranium Ore

The efficiency of uranium recovery is influenced by the mineralogical characteristics of the ore. In particular, the bulk composition affects reagent consumption and ferric generation, while the uranium mineral composition and mode of occurrence influences the uranium dissolution (Lottering, *et al*, 2008).

Uranium minerals may be termed primary or secondary, depending upon their degree of oxidation and origin. Tetravalent uranium (primary) is principally found in the minerals uraninite and its amorphous form, pitchblende, which occurs in many of the world's deposits. Uraninite contains uranium as an oxide, approximately of the formula UO_2 , but generally having a composition somewhere between UO_2 and UO_3 (Merritt, 1971).

Uranium mineralisation occurs as inclusions in quartz, feldspar and biotite, as well as interstitially in these minerals or along cracks within the grains (IAEA, 1993). Approximately 40% of the uranium and most of the economic ore occurs as secondary U^{6+} minerals formed by oxidation and supergene enrichment (Misra, 2000). In Southern Africa, the predominant uranium minerals are uraninite (UO_2), various hydrated secondary oxides ($UO_3 \cdot nH_2O$) and, as has been more recently recognized, brannerite (UTi_2O_6). In addition, minor amounts are found as uraniferous zircon, monazite and other rarer minerals (Nicol, 1981).

According to Schreuder and Roesener (1992), uraninite is the principal uranium mineral at Rössing Uranium Ltd; although some betafite and beta uranophane are also present. Studies conducted by Rössing Uranium Ltd on the run of mine (ROM) ore have shown that primary uranium minerals (uraninite and betafite) which are confined to alaskite, and the secondary mineralisation (uranophane) both occur in alaskite and the surrounding host rocks of the Khan and Rössing formations. The study also revealed that the primary mineral which is

predominantly uraninite (UO₂) occurs as grains ranging in size from a few microns to 0.3 mm, with the majority in the 0.05 to 0.1 mm fraction. In spite of the general small grain size of uraninite (0.05 to 0.1 mm), it is nevertheless accessible to leaching at a much coarser grind than the expected liberation size, because in many instances it occurs along cracks in the quartz and feldspar and between flakes of biotite (Vernon, 1981).

2.2 Chemistry of uranium leaching

Uranium can be recovered from its ores using a hydrometallurgical process. Depending on the nature of the ore, either an acid or an alkaline medium can be used as a lixiviant. The first stage of recovery is normally leaching which aims at selectively dissolving uranium and leaving other components in the ore. The Rössing Uranium plant uses sulfuric acid as a lixiviant to extract uranium under oxidising conditions in stirred vessels. Dilute sulfuric acid is the most widely used leachant for the extraction of uranium from its ores. However, alkali and ammonium carbonates solutions are preferred leachants for ores associated with large quantities of acid consuming components such as carbonates (dolomite and calcite) and oxide (magnetite) (Eligwe, *et al.*, 1982). This is the case for Paladin Energy's Langer Heinrich plant which uses an alkaline process.

In the conventional acid or alkaline leaching of uranium ores, compounds of hexavalent uranium (secondary) dissolve readily while those of tetravalent uranium must first be oxidised by a suitable oxidant to the hexavalent state before dissolution occurs (Merritt, 1971). In literature, Merritt (1971) suggested that when sulfuric acid ionizes in solution, it forms sulfate, bisulfate and hydrogen ions, which when reacting with hexavalent uranium produces uranyl sulfate and the complex uranyl sulfate ion as follows:



Depending on the acid concentration, temperature and other variables in the system, the dissolved uranium may occur in any of the above forms. Hennig *et al.*, (2007) reported that in acidic conditions, thermodynamic speciation reveals three sulfato species, UO₂SO_{4 (aq)}, UO₂

$(\text{SO}_4)_2^{2-}$ and $\text{UO}_2(\text{SO}_4)_3^{4-}$ and at $\text{pH} > 5$ different ternary sulfato complexes with bridging hydroxide and oxide occur.

Tetravalent uranium requires oxidation before it can dissolve in sulfuric acid. The oxidation of tetravalent uranium to the soluble hexavalent form is commonly effected by ferric iron that occurs in the ore or that is added during leaching (Nirdosh, 1985). The reaction may be represented as follows:



It can be seen that acid is not consumed in this reaction but required to maintain a pH below 2 to avoid ferric hydrolysis. However, acid is consumed when ferrous ion have to be oxidised to ferric ion again by pyrolusite as shown in the following reaction:

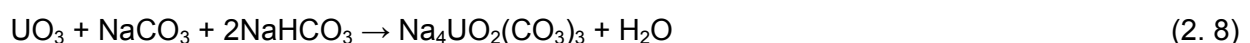


Sodium permanganate (NaMnO_4) can also be used to oxidise ferrous resulting in the following reaction:

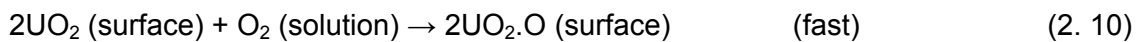
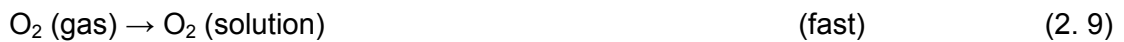


There are other oxidants such as sodium chlorate (NaClO_3) that can be used to oxidize ferrous ion that may require more acid. Oxidants act indirectly by converting ferrous sulfate formed due to reduction by U(IV), the dissolution of iron minerals in the ore or iron introduced during grinding, into ferric sulfate. A Fe(III) concentration of about $0.018 - 0.036 \text{ mol dm}^{-3}$ is usually considered adequate for the effective dissolution of uraninite (Laxen, 1973). However, in industry, plants operate at much higher concentrations than that, mainly due to improved leaching kinetics achievable at higher concentrations.

In an alkaline leach, the following reactions describe the chemistry that takes place:



In this case, O_2 is used as the oxidant as UO_2 has to be oxidized before it can be dissolved by the carbonates. Before tetravalent uranium can be oxidized, the gaseous oxygen will first have to dissolve into the solution and then adsorbed on the surface of UO_2 . Merritt (1971) reported that both of these reactions are relatively fast and that the slow one is the rate determining reaction and is the rearrangement of the adsorbed O_2 on the UO_2 with the accompanying oxidation to UO_3 . Merritt (1971) listed these three reactions as follows:



Data have shown that the overall rate of the reactions is directly proportional to the UO_2 surface area and to the square root of the oxygen partial pressure (Merritt, 1971).

Eh – pH diagrams have been used to summarise the thermodynamic conditions required to keep metals in solution. The diagram below is one drawn for U-S- H_2O system at $25^\circ C$.

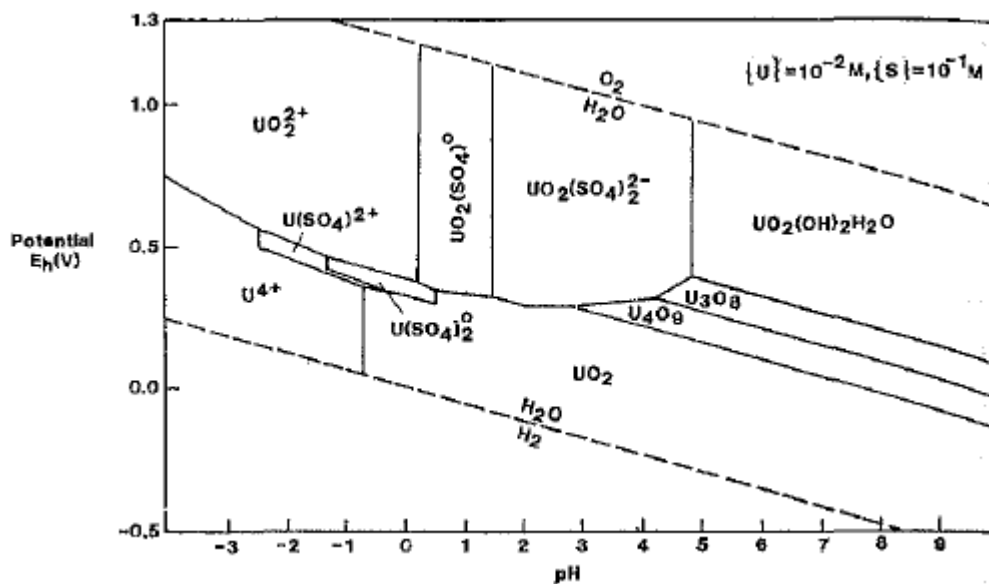


Figure 2. 1: Eh/pH diagram of U-S- H_2O system at $25^\circ C$. Source: (Hayes, 2003)

The diagram consists of a series of domains of stability in which only certain species are thermodynamically stable. In order to convert one species to another, one must move across the lines bordering the domains (Nicol, 1981). It can be observed that in order to leach UO_2 , it is required to operate at low pH. UO_2 can be oxidised to uranyl ion (UO_2^{2+}) at a potential above

0.4V in acid region. This information only tells us the thermodynamic possibilities; it does not say anything about how fast these reactions will take place.

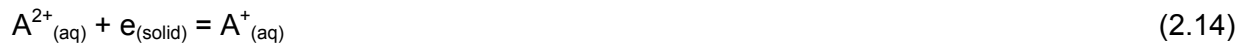
Experimental work would have to be carried out to determine the rate at which the reactions occur. This normally involves taking samples at predetermined times during the leach to determine extraction. Extraction is then plotted against time. The rates are obtained by taking tangents to the curve at selected times. If it is possible to measure the extent to which the reaction has occurred over a period of time during which the concentrations of the reactants are effectively constant (Burkin, 2001), then these measurements will give the average reaction rate under the conditions used. The rate is usually higher in the beginning and decreases towards the end. This may be attributed to the decreasing area of the solid as the reactants are usually in excess.

2.2.1 Proposed mechanisms of uranium dissolution

Following on the fundamental studies of the dissolution of uraninite carried out at the National Institute for Metallurgy in the 1970's, it's now generally accepted that the electrochemical model of the leaching process can be used to both qualitatively and quantitatively describe the leaching behavior of UO_2 (Nicol, 1981). This is to say that uraninite dissolution reaction is of an electrochemical nature which involves transferring of electrons. Dissolution and corrosion reactions often result in a change in oxidation state, and hence these reactions can be separated into an anodic half-reaction and cathodic half-reaction (Crundwell, 2013). The dissolution of UO_2 in the equation (2.5) can be said to be the sum of the following half reactions;



Uraninite is being oxidised while at the same time ferric ion are reduced to ferrous ion. Here two half-cell reactions occur simultaneously by electron transfer across the interface between the solid and the solution. UO_2^{2+} can then form complexes as shown in equations (2.2 – 2.4) in accordance with what was reported by Burkin (2001) that it has been accepted that oxidation of tetravalent to hexavalent takes place before a uranium ion transfers to the aqueous phase. Crundwell (2013) explains the simple electron-transfer reaction as one in which a redox couple (A^{2+}/A^+) in solution interacts with an electron in an inert solid:



Studies done by Kesler (1978) at Rössing Uranium plant indicates that Fe(III)/Fe(II) couple plays a dominate role as the electron acceptor for the oxidation of tetravalent to hexavalent uranium. The oxidant (pyrolusite) is added to reoxidise Fe(II) ion to Fe(III) ion so that there are always Fe(III) ion in the solution for the reaction to continue. A relationship between the Fe(III)/Fe(II) ratio and oxidation-reduction potential (ORP) at Rössing Uranium plant has been established. ORP can now be used as the means of monitoring the Fe(III)/Fe(II) ratio in the leach tanks. Ring (1980) used the Nernst equation to show this relationship. Ring (1980) reported a linear relationship between \log Fe(III)/Fe(II) concentration ratio and redox potential which implies that monitoring the redox potential would enable one to determine the ratio of Fe(III)/Fe(II) up to ratios of 100. A control system based on this relationship can easily be employed in a system as ORP is easy to measure.

The relationship between Fe(III)/Fe(II) ratio and ORP observed with the Rössing plant solutions also shows a linear correlation as reported by Ring (1980) when the logarithm of Fe(III)/Fe(II) is plotted against ORP. This relationship was established by measuring the ORP and determining the Fe(III)/Fe(II) ratio by titration on Rössing Uranium plant solutions. The relationship was then modeled and the model is shown in equation 2.15. The model can be used to predict the Fe(III)/Fe(II) ratio by measuring the ORP in the leach tanks. The Rössing leach plant typically operates between Fe(III)/Fe(II) ratios 2 and 4.

$$\text{ORP (mV)} = 435 - 28 \ln \frac{[\text{Fe(II)}]}{[\text{Fe(III)}]} \quad (2.15)$$

Equation 2.15 is similar (they all show a linear relationship between Fe(III)/Fe(II) and ORP) to the equation used by Ring (1980) and can yield the same results, as shown in figure 2.2. The ORP was measured using a 3M KCl Ag/AgCl electrode.

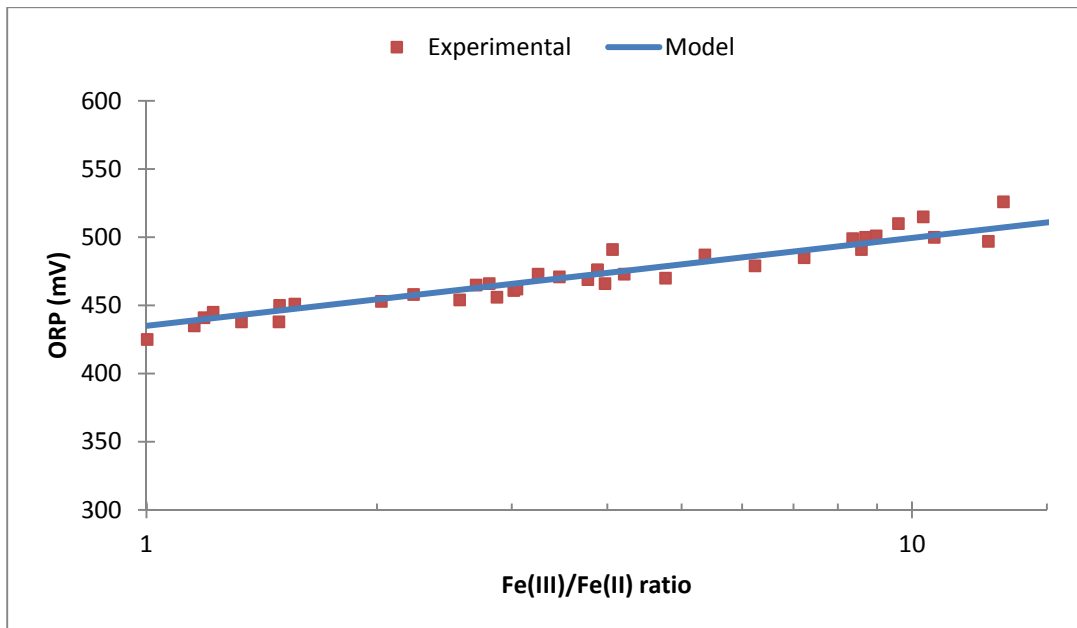
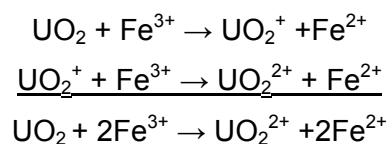


Figure 2. 2: Experimentally determined relationship between Fe(III)/Fe(II) ratio and ORP of Rössing plant solutions (3M KCl Ag/AgCl electrode)

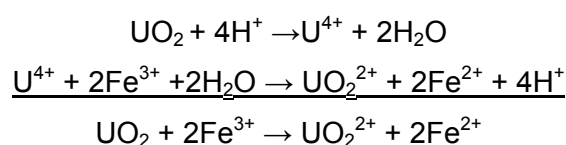
Burkin (2001) also emphasises that uraninite dissolution is of an electrochemical nature. He showed that the uraninite dissolution reaction satisfies two conditions required for a reaction to be of electrochemical nature. The first is that the overall reaction demonstrates in all respects that it is a sum of the two half-cell reactions (2.12) and (2.13) in the case of UO_2 oxidation by ferric ion. The second is that the oxidation of the mineral e.g. UO_2 should follow the same pathway regardless of the source of the potential i.e. from a potentiostat or from a chemical oxidant in solution.

Other mechanisms to explain UO_2 dissolution were suggested. Spitsyn *et al.*, (1965) suggested the following two mechanisms:

Mechanism 1



Mechanism 2



Mechanism 1 only shows the oxidation of UO_2 to UO_2^{2+} by Fe(III) ion. The authors did not show the next step that would presumably involve UO_2^{2+} complexing with SO_4^{2-} according to equations (2.2–2.4). This will mean that oxidation occurs before dissolution which is in accordance with Burkin (2001). The second mechanism however suggests that UO_2 dissolution takes place before oxidation. Mechanism 2 cannot hold as Spitsyn *et al.*, (1965) recorded that only 1.76% of UO_2 can dissolve in $0.122 \text{ mol dm}^{-3} \text{ H}_2\text{SO}_4$ at 70°C . This is not unexpected considering that the Pourbaix diagram shown earlier indicates that the U^{4+} will only be stable for $\text{pH} < -1$. Because of this, it can be assumed that the second mechanism does not play a major part in the process, and UO_2 oxidation by Fe(III) ion proceeds according to the first mechanism (Spitsyn, *et al*, 1965).

Although the hydrogen ion does not participate in the uranium oxidation, the effect of the acid concentration in solution is undoubtedly one of the determining factors when this reaction proceeds during acid leaching of uranium from the ores (Spitsyn, *et al*, 1965). Fe(III) ion requires low pH to stay in solution. Acid is required in the reoxidation of Fe(II) ion to Fe(III) ion by pyrolusite as shown in equation (2.6).

Sunder and Shoemith (1991) have summarized the dissolution of UO_2 to consist of five stages as shown in figure 2.3.

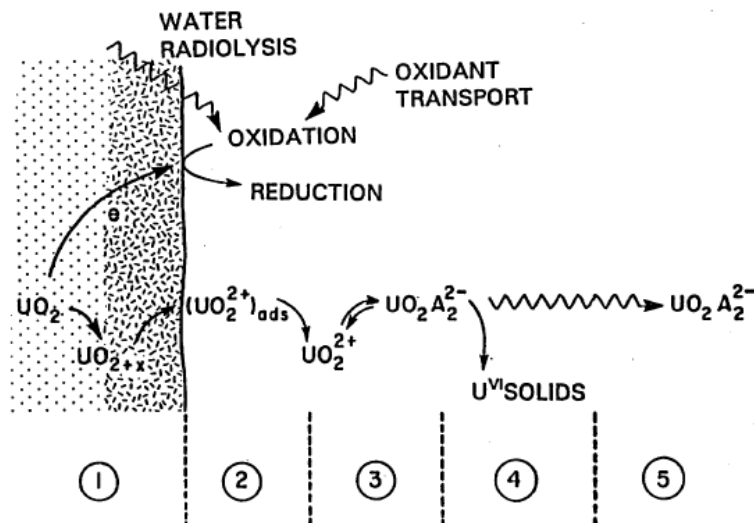


Figure 2. 3: Schematic representation of processes occurring during oxidative dissolution of UO_2 in a geological Vault. Source: (Sunder and Shoemith, 1991).

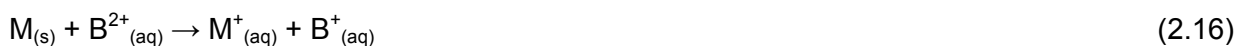
Sunder and Shoesmith (1991) explained these steps as follows;

- Stage 1 in this figure represents the primary step of UO_2 oxidation and the formation of an oxidised transient layer on the UO_2 surface.
- Stage 2 represents the formation of the UO_2^{2+} ion on the oxidised transient layer and its subsequent dissolution.

These two stages (1 and 2) are determined by the surface redox conditions, i.e., the balance of kinetics between the anodic reaction (oxidation of UO_2) and the cathodic reaction (reduction of the oxidizing agent).

- The complexation of the uranyl ion in the slurry, represented by stage 3 in Figure 2.3, may be said to be determined by the leach solution composition. Complexation can have a direct influence on dissolution (stage 2), as well as affecting stages 4 and 5.
- Stage 4 represents the precipitation of secondary phases. It may affect dissolution, depending upon the relative location of the precipitation site and the UO_2 surface.
- Stage 5 represents the transportation of uranium species and will be influenced by slurry composition, the presence of colloids, and the density of the pulp and the agitation in the leach vessel.

An accurate understanding of the behavior of the kinetics of dissolution is required in order to interpret the complex behaviour of leaching reactors, and to optimise the performance of a hydrometallurgical operation (Crundwell, 2013). Crundwell (2013) looked at the dissolution of a mineral M in an aqueous solution containing the oxidant B^{2+} . He suggested that a general kinetic mechanism for oxidative leaching for the reaction,



can be expressed as:

$$r_{diss} = K_a \left(\frac{K_c [B^{2+}]}{K_a + K_c^1 [B^+]} \right)^{0.5} \quad (2.17)$$

where r_{diss} represents the rate of dissolution and K_a and K_c are the rate constants for the forward (anodic dissolution) and backward (cathodic deposition) reactions, respectively. K_c^1 is the rate constant for the backward reaction that is dependent on the potential difference across the solid–solution interface.

The dissolution rate r_{diss} , can be expressed in terms of the oxidant as in equation (2.17) as the rate at which electrons are donated by the oxidant is equal to the rate that they are accepted by the mineral surface. Applying the general equation (2.17) to UO_2 being oxidized by ferric, Nicol et al. (1975) came up with the following general kinetic expression for uraninite:

$$r_{diss} = K_a \left(\frac{K_c [Fe^{3+}]}{K_a + K_c^1 [Fe^{2+}]} \right)^{0.5} \quad (2.18)$$

This implies that the rate of dissolution of uraninite is a function of the concentration of the oxidant, in this case, Fe(III). This is supported by Ram (2011) who reported an approximately linear dependence of UO_2 dissolution on total iron at OPR values between 460 and 565mV, Ag/AgCl electrode. Crundwell (2013) suggested that equation (2.17) has two limiting forms:

i) If $K_a \gg K_c^1 [B^+]$, then the rate of dissolution is given by the following equation:

$$r_{diss} = (K_a)^{0.5} (K_c [B^{2+}])^{0.5} \quad (2.19)$$

ii) If $K_a \ll K_c^1 [B^+]$, then the rate of dissolution is dependent on the ratio of the concentration of the oxidant, B^{2+} , and its reduced form B^+ , and the corresponding expression for the rate of reaction is given by:

$$r_{diss} = K_a \left(\frac{K_c [B^{2+}]}{K_c^1 [B^+]} \right)^{0.5} \quad (2.20)$$

If the K_a and $K_c^1 [B^+]$, are of similar magnitude, then the full form of equation (2.17) is required. Both forms apply in uraninite leaching as Nicol and Needes (1975) noted that at higher concentration of Fe(III), the Fe(II) becomes negligible, the dissolution rate will take the form of the equation (2.19) and where the concentration of Fe(II) is not negligible, the dissolution rate will depend on the ratio of Fe(III)/Fe(II) which is the form of equation (2.20).

Studies done by Rössing Uranium plant show that extraction is directly related to the Fe(III)/Fe(II) ratio. It was found that the increase in the Fe(III)/Fe(II) ratio results in increased extraction. Based on this finding, one may propose that the dissolution rate at Rössing plant will take the form of equation (2.20) as studies conducted showed that the rate depended on the Fe(III)/Fe(II) ratio and this may be expressed as:

$$r_{diss} = K_a \left(\frac{K_c [Fe^{3+}]}{K_c^1 [Fe^{2+}]} \right)^{0.5} \quad (2.21)$$

2.2.2 Oxidants

Redox potential is the most important parameter governing the dissolution of UO_2 (Sunder and Shoesmith, 1991). It is recorded in literature by Nicol (1981) that there exist a number of different oxidants that can accept electrons from uraninite and therefore they may be used in the leaching of uraninite. These include ferric ion (Fe^{3+}), pyrolusite (MnO_2), chlorine (Cl_2), chlorate ion (ClO_3^-), hydrogen peroxide (H_2O_2), persulfate ion ($S_2O_8^{2-}$), and oxygen (O_2). In the ferric sulfate system, the chemical oxidants act indirectly by reoxidising the ferrous ion to the ferric state in order to maintain the required redox potential (Merritt, 1971) therefore the actual uraninite oxidation is due to the Fe(III) ion.

The most common commercially used oxidants are pyrolusite (MnO_2) and sodium chlorate ($NaClO_3$), but these introduce Mn^{2+} and Cl^- ions into the process liquors, which have potential adverse downstream environmental and uranium recovery impacts, respectively (Ring and Ho, 2007). Though the oxygen/water half-cell may have a more positive potential than that of Fe(III)/Fe(II) half-cell, the latter is used. Reduction of dissolved oxygen on the UO_2 surface is a very slow reaction because of the necessity to break the strong O-O bond (Luht, 1998). This may suggest that the Fe(III)/Fe(II) half-cell is preferred as it has relatively faster kinetics compared to oxygen/water half-cell.

The other considerations that will influence the choice of oxidant are reported by Ho and Quan (2007) as the types of uranium and gangue minerals, reagent costs and environmental waste treatment considerations. Added to this, is the consideration of the effect the oxidant would have on the downstream processes. At the Rössing Uranium plant for example, which employs ion exchange as the means of recovering uranium from the pregnant solution, high concentrations of chlorides have been shown to reduce loading of uranium on resin. As a result, $NaClO_3$ would not be a suitable oxidant for the Rössing Uranium leach plant.

Other oxidants such as hydrogen peroxide can also be used. Nicol (1981) suggests that H_2O_2 suffers from the disadvantage that it decomposes by disproportionation rapidly in acid solutions, particularly in the presence of some metal ion, notably ferric ion. This may be the reason why it is not commonly used in uranium plants despite the fact that it is chemically attractive. Although thermodynamically much more powerful, oxygen ($E^\circ = 1.23V$ vs SHE) is only capable of achieving measurable dissolution rates at high temperatures and pressures

while ferric/ferrous half-cell ($E^\circ = 0.77V$ vs SHE) can produce satisfactory extraction at ambient temperatures (Nicol, 1981). This may be the reason why the Rössing Uranium plant prefers the latter over the former.

Ho and Quan (2007) studied the oxidation of iron by using SO_2/O_2 for leaching uranium. This study used both O_2 and air as a source of oxygen. The oxidation of Fe(II) ion requires both SO_2 and O_2 as shown below.



The pH was controlled by the addition of sulfuric acid. In another parallel study, Ho and Quan (2007) had done, they used sodium sulfite as the source of SO_2 in which sodium hydroxide was used to control the pH. They found that the oxidation rate of Fe(II) ion was the same for both cases. They further found out that the ratio SO_2/O_2 had an effect on the rate of Fe(II) ion oxidation. When the ratio increased, meaning more SO_2 , the environment became reducing which resulted in the decrease of the Fe(II) ion oxidation rate. They concluded that uranium leaching using SO_2/O_2 as an oxidant was successful on the laboratory bench scale.

Prior to Ho and Quan (2007) study, Ford (1993) reported that the auto-oxidation process which introduced sulfur dioxide and air into a solution of ferrous sulfate to produce the required ferric ion and additional acid was successfully used in the 1980s at Hartebeestfontein, but it was stopped due to availability of cheaper sources of pyrolusite. In this process, Ford (1993) reports that the calcine from the roasting of pyrite was treated with concentrated sulfuric acid in Broadfield mixers. The resulting slurry was contacted with sulfur dioxide in flotation cells and yielded high concentrations of ferric ion. These results again show that other oxidants besides MnO_2 and $NaClO_3$ can be used successfully depending on the downstream processes.

2.3 Operating parameters of interest

Sunder and Shoesmith (1991) reported that chemical species dissolved in the slurry may have an influence on the kinetics of oxidative dissolution of uraninite by directly being involved in the dissolution reaction, by changing the redox conditions that control dissolution or by forming a transport barrier that inhibits the transportation of the oxidant to, or dissolution product from, the solid surface. Other factors that will control the uranium leaching kinetics are dealt with below.

2.3.1 Pulp density

Pulp density is one of the parameters that are closely monitored during agitation leaching. The reasons for monitoring pulp density may range from the ability to suspend the particles in the vessel to economic considerations. Merritt (1971) reported that leaching is a diffusion process with the leaching rate proportional to the reagent concentration, the temperature, the surface area of the solid, and the rate of diffusion through the solution layer adjacent to the solid surface. Therefore the diffusion coefficient will decrease with the increased viscosity in the medium. The high viscosity in this case is caused by a high concentration of slimes (high pulp density). In an instance where leaching is a diffusion controlled process, pulp density plays a role in leaching kinetics.

A high pulp density may result in a reduced leaching rate and will cause the leaching rate to be diffusion controlled instead of reaction controlled as suggested by Merritt (1971). A lower pulp density may result in higher requirements for reagents to be able to maintain the required concentration of reactants. On the other hand, operating with a high slurry density reduces the volume of the leaching circuit required to obtain a desired residence time and reduces reagent consumptions required to achieve the desired reagent concentrations (Ajuria, *et al*, 1990). Due to the factors mentioned above it is therefore necessary to determine the optimum pulp density to operate at. The optimum pulp density in the leaching circuit is usually the maximum possible, while still permitting sufficient fluidity in the pulp to avoid poor contact between the liquid and the surfaces of the solids (Merritt, 1971).

Tamrakar *et al.*, (2010) studied the effect of pulp density on uranium leaching. They considered the following pulp densities, 40%, 50%, 60% and 70% solids in their study. The results they found are shown in figure 2.4.

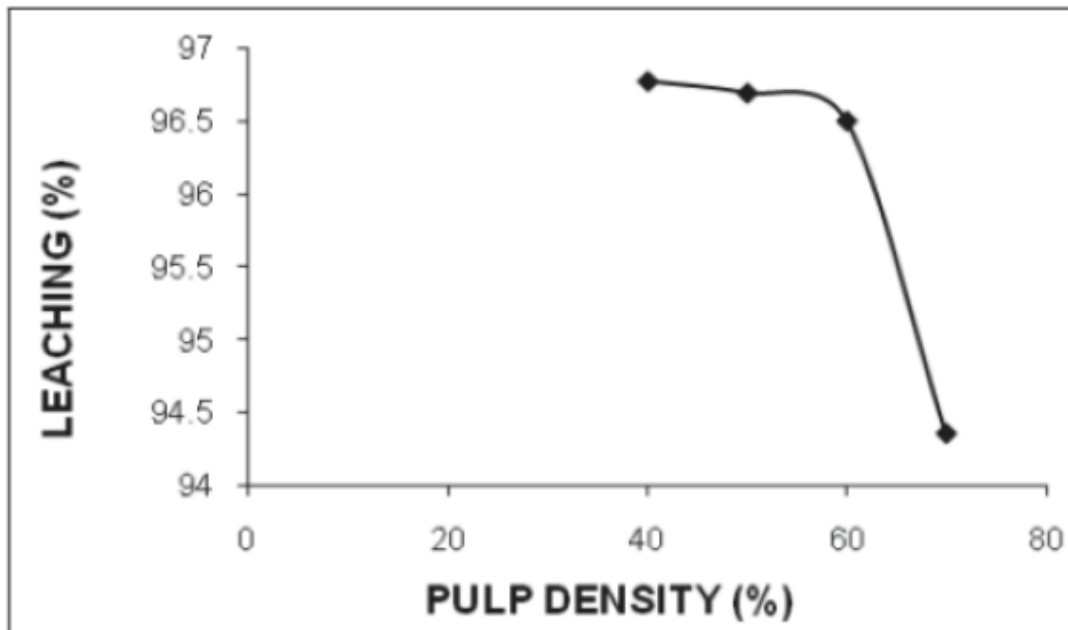


Figure 2. 4: Effect of pulp density on uranium leaching. Source: (Tamrakar *et al.*, 2010)

In this study they concluded that 60% solids was the optimum in terms of the maximum possible pulp density that gives a proper solid and liquid contact with better leachability. The graph also shows a steep decrease in % leaching between 60 and 70% solids which may be due to the decreased diffusion coefficient as suggested by (Merritt, 1971). The optimum pulp density would differ from ore to ore. The Rössing Uranium plant for example, targets 70% solids.

2.3.2 Iron concentration

The role of iron in uranium leaching in acidic conditions is very important. Ferric ion act as the principal oxidant of tetravalent uranium in acid leaching circuits (Tamrakar *et al*, 2010). Tests with South African ores showed that leaching for 24 h at 64°C with a ferric ion concentration of 0.125 M achieved an extraction of uranium of 93 per cent compared with the 80-85 per cent obtained by conventional leaching using manganese dioxide as an oxidant (James, 1976). But an oxidant such as pyrolusite is required to reoxidise the reduced Fe(II) ion to Fe(III) ion.

The Rössing Uranium plant has successfully used pyrolusite and iron as oxidants. Early plant performance data showed that high ferric ion concentrations were necessary to achieve optimum uranium extraction. Under normal conditions, ferric ion concentration was generally

only 0.0143 to 0.0269 M. Increasing this level to 0.0537 M improved average uranium extraction by 4 to 5 % (percentage points). Mineralogical examinations showed that extraction was increased because of the additional dissolution of uraninite, indicating that the additional ferric ion concentration did not improve the recovery from the refractory mineralization.

Ram *et al.*, (2011) studied the effect of Fe(III) ion concentration on uranium dissolution under conditions of constant Fe(II) ion concentration. This is essentially the effect of ORP on the dissolution of UO_2 . Their study used UO_2 which was prepared from uranyl acetate ($UO_2(CH_3COO)_2 \cdot 2H_2O$). The Fe(III) ion was used as an oxidant and $NaClO_3$ was used to maintain the required ORP in acidic conditions. The results are shown in figure 2.5.

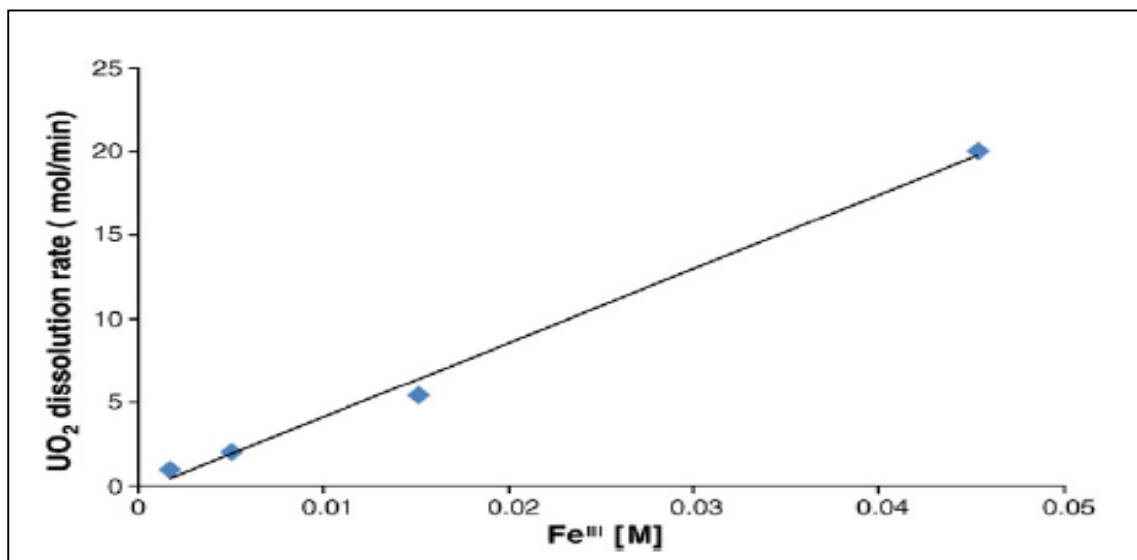


Figure 2. 5: Plot of UO_2 dissolution rate versus $[Fe(III)]$ at constant $[Fe(II)]$ ($5.04E10^{-3}$ M). Source: (Ram *et al*, 2011)

The study found that the rate of uraninite dissolution was dependent on Fe(III) ion concentration. The dependence was found to be linear in nature as shown in figure 2.5. The rate increased with increasing Fe(III) ion concentration (increasing ORP) at constant Fe(II) ion concentration. This result supports Dutrizac and MacDonald (1974) who suggested that increasing the concentration of Fe(III) ion could improve leaching rates. This however, is only possible when the Fe(II) ion produced is reoxidised during leaching and recycled. As a result, many uranium processing plants that use Fe(III) ion as an oxidant also use pyrolusite or some sort of oxidant at the same time to achieve this Fe(II) ion to Fe(III) ion cycle.

Similar findings are also reported by Nicol and Needes (1975), indicating that the dissolution rate was also affected by the presence of Fe(II) ion, but the form of the dependence was determined by the Fe(III)/Fe(II) ratio. Where the concentration of Fe(II) ion was negligible, which is the most common situation in commercial leaching operations, the rate of leaching was independent of the Fe(II) ion concentration. Therefore the high concentration of Fe(III) ion in solution is vital for an improved leaching rate.

Ram *et al.*, (2011) also studied the dependency of UO₂ dissolution rate on total Fe at 460 mV vs Ag/AgCl. As shown in figure 2.6, the study found that the dependency of UO₂ dissolution rate on iron concentration was established to be linear except over the lower range of Fe concentration.

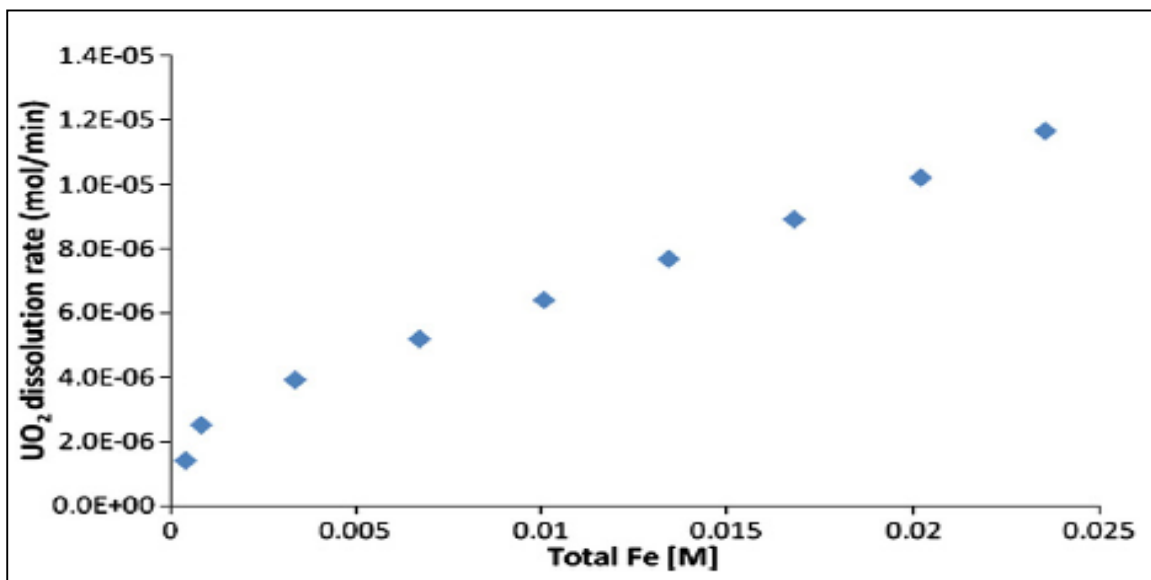


Figure 2. 6: UO₂ dissolution rate vs. total Fe for solutions at an ORP of 460 mV. Source: (Ram *et al.*, 2011)

In the same study, Ram *et al.*, (2011) also looked at the influence that iron concentration has on uranium leach kinetics over a range of ORP values. The results are shown in figure 2.7 below.

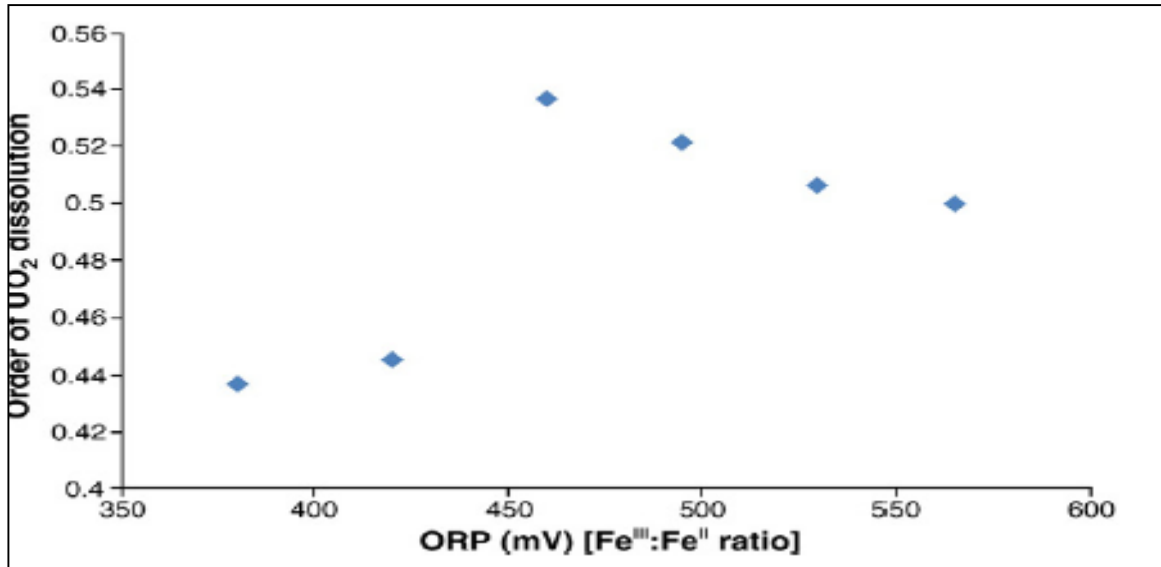


Figure 2. 7: Order of UO₂ dissolution with respect to Fe vs. solution ORP Ag/AgCl electrode.
Source: (Ram *et al.*, 2011).

They found that the order of UO₂ dissolution has a different dependency on the iron concentration for different ORP values. This dependence can be seen in mechanism 1 where it is shown that the dissolution of UO₂ is effected by Fe(III) ion. In the ORP range of 460 – 565 mV vs Ag/AgCl, they reported a strong dependency of order of UO₂ dissolution on iron concentration. In this range, most of the Fe will be in Fe(III) state. So the increase in iron concentration implies an increase in Fe(III) ion, which is responsible for UO₂ oxidation Nicol (1985). At 420 mV and below, the dependency of the order of UO₂ dissolution was significantly lower. At this ORP (420 mV) Fe(II) ion is the predominant species and therefore the increase in iron concentration will not result in an increase in the dissolution rate.

Nirdosh (1985) reported that a concentration of Fe(III) ion as low as 0.01 M is effective for obtaining nearly 95% dissolution of the uranium. Therefore there is no additional advantage in using a concentration of ferric ion greater than 0.02 M. Gogoleva (2012) conducted similar studies on brannerite (UTi₂O₆)¹ by looking at the influence of the concentration of Fe(III) ion between 0.0025 to 0.10 M on UTi₂O₆ dissolution. The results are shown in the figure below.

¹ Brannerite contains U⁴⁺ which has the same oxidation state as that contained in uraninite. Both U⁴⁺ from brannerite and uraninite must first be oxidised to hexavalent state in order to dissolve them. Conclusions drawn from one of them maybe useful to understand the other.

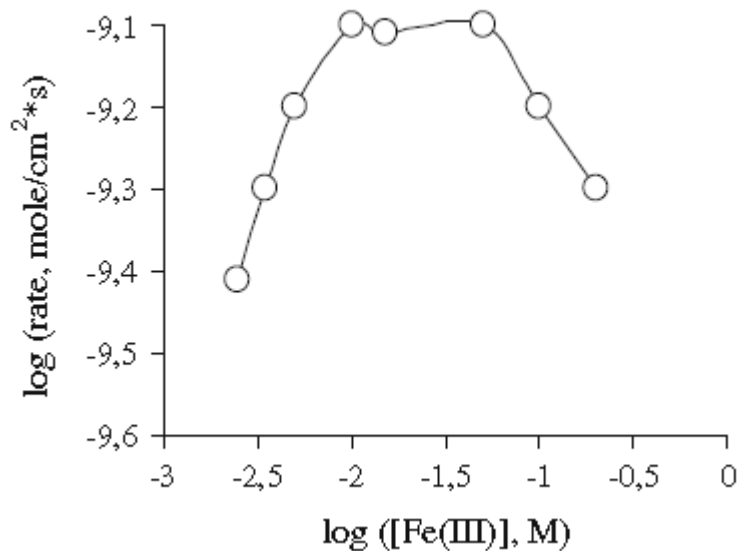


Figure 2. 8: The effect of Fe(III) concentration on the leaching rate of brannerite ore. [H₂SO₄] initial = 0.5 M; temperature: 70 °C; rotation stirrer speed: 500 rpm. Source: (Gogoleva, 2012).

The results from this study showed an increased dissolution rate with an increased concentration of Fe(III) ion to 0.1 M. However, the rate decreased above a concentration of Fe(III) ion of 0.1 M. The decrease in the dissolution rate was proposed to be due to the precipitation of hydrates such as Fe₂O₃.H₂O on the surface of the ore (Gogoleva, 2012). In this case the access path of reagents to the reacting site is blocked and this may explain the decrease in the rate of dissolution. When the concentration of Fe(III) ion had risen above 0.1 M, the surface of the leached sample was observed to have a passive film on the leached ore surface (Gogoleva, 2012). These studies were conducted using a brannerite sample where uranium (IV) from brannerite must be oxidized to a hexavalent state in order to be dissolved, just like in uraninite ore.

2.3.3 Oxidation/reduction potential

The amount of oxidant added to a leach circuit is usually controlled to achieve a target potential in the uranium slurry so that the uranium (IV) is oxidised. The potential operating range for sulfuric acid leaching is typically 450 - 525 mV vs Ag/AgCl/ 3M KCl (IAEA, 1993).

Ram *et al.*, (2011) observed that the concentration of Fe(III) and Fe(II) ion and solution ORP are very closely related, with solution ORP defined by Fe(III)/Fe(II) ratio. As such the influence that Fe(III), Fe(II) and ORP have on the rate of UO₂ dissolution cannot be isolated as changing

either the concentration of Fe(III) ion or Fe(II) ion in the solution will also lead to a change in solution ORP.

Iron concentration is the sum of concentrations of Fe(III) and Fe(II) ion in the system. The increase in iron concentration at constant ORP should therefore be seen as the proportionate increments in concentrations of Fe(III) and Fe(II) ion. This is so because Fe(III)/Fe(II) ratio has an influence on the ORP of the system. This can be seen when one takes the Nernst equation for the Fe(III)/Fe(II) half-cell reaction into account, the thermodynamic equation may be written as:

$$E = E^0 - 0.059 \log \frac{[Fe(II)]}{[Fe(III)]} \quad (2.23)$$

where E^0 is the standard reduction potential.

From equation 2.23, one can see that the higher the concentration of Fe(III) ion for a given Fe(II) ion concentration, the higher the potential. A high value of ORP implies that the system has a high oxidising power. However, a higher ORP does not automatically indicate an improved dissolution rate. This is because the concentration of Fe(III) has an influence on the dissolution rate. A high ORP value can be achieved by even low concentration for both Fe (III) and Fe(II).

2.3.4 Effects of pH

A principal requirement of acid sulfate leaching is the maintenance of a free acid concentration sufficient to keep uranium and ferric ion in solution without dissolving an excessive amount of associated gangue minerals (Bhargava, *et al.*, 2015). Ferric ion leaching solutions are sensitive to pH changes. Sufficient acid is required to maintain pH of less than about 2.5 to prevent the precipitation of ferric ion as the hydroxide and preferably below 2.0, which favours the formation of the most effective ferric complex, $FeSO_4^+$ (Nicol *et al.*, 1975). In general, an increase in H_2SO_4 concentration decreases the pH, which in turn makes it possible for Fe(III) ion required for dissolution to stay in solution. This has an effect of increasing the rate of uranium dissolution as reported by Gogoleva (2012) as well as Eligwe and Torma (1982).

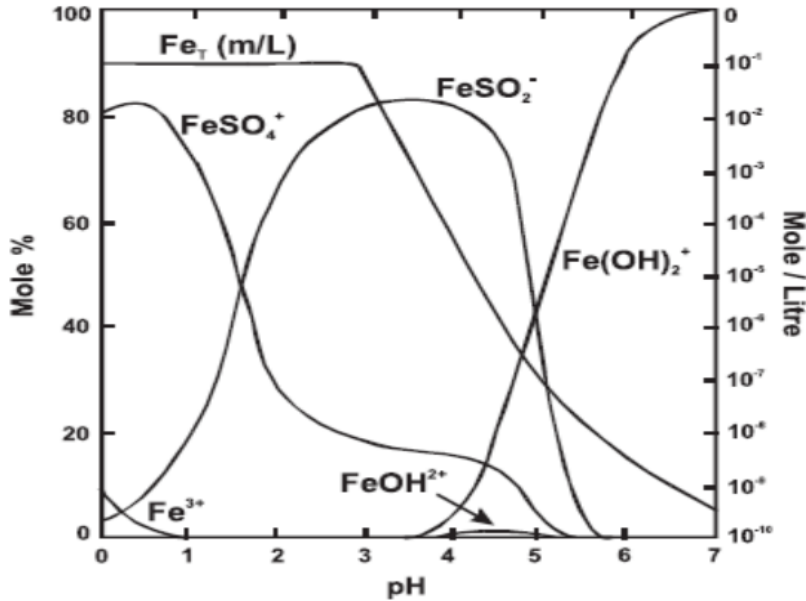


Figure 2. 9: Equilibrium iron species existing in a solution containing 0.1MFe³⁺ and 0.5M total sulfate at 25 °C. Source: Bhappu et al., (1969).

Figure 2.9 shows how increase in pH results in the decrease in Fe(III) ion in solution. This may explain why the increase in pH would result in decreased uranium extraction. Ram *et al.*, (2013) investigated the effect of increasing the concentration of sulfuric acid on uranium extraction rates. The experimental conditions were [H₂SO₄] = 0.015 - 0.7M, Total Fe= 8.83E10⁻³M; ORP= 460 mV vs. Ag/AgCl and temperature= 50⁰C. The results indicated that there was no significant effect on the rate. Bhargava *et al.*, (2015) cited many researchers that all seem to agree that there exist a pH value below which the increase in sulfuric acid concentration or lowering the pH would not have an effect on the uranium dissolution rate.

Gogoleva (2012) studied the effect of increasing H₂SO₄ concentration at a constant temperature on UTi₂O₆ dissolution. The brannerite ore used in this study was obtained from a uranium deposit at Jakutia (Russia). The H₂SO₄ concentrations were varied from 0.1 to 2.0 M. Temperatures of solutions were maintained at 70⁰C. The results are shown in figure 2.10 below.

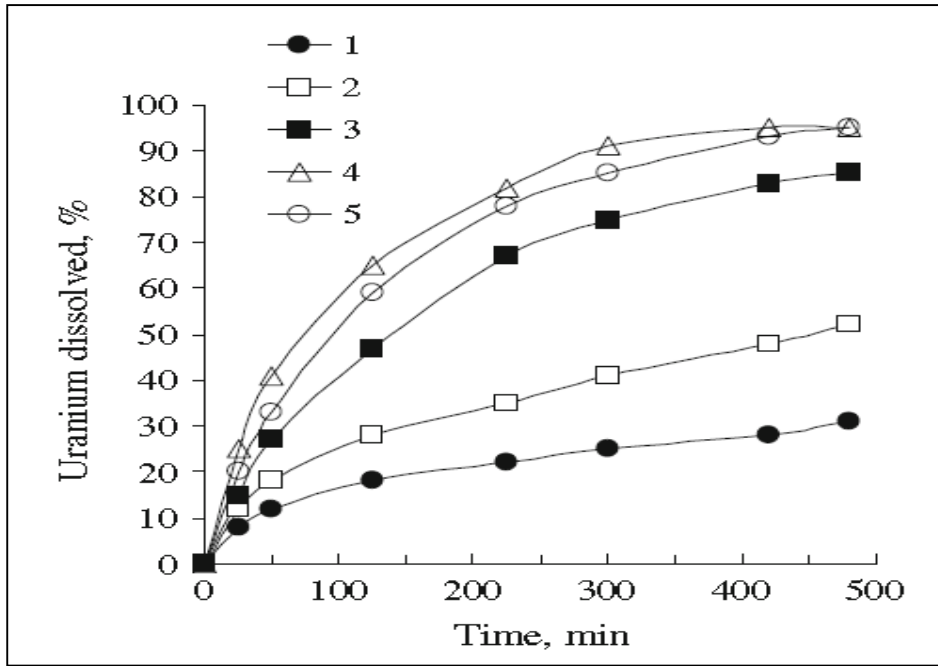


Figure 2. 10: The amount of uranium dissolved (%) from ore as a function of time at various H_2SO_4 concentrations, M: 0.1 (1), 0.2 (2), 0.5 (3), 1.0 (4), 2.0 (5). Temperature: $70\ ^\circ C$; $M; [Fe(III)]_{initial} = 0.01\ M$, particle size: $53\text{--}74\ \mu m$. Source: (Gogoleva, 2012)

It was found that the leaching rate increased with an increase in the concentration of H_2SO_4 . This can clearly be seen in figure 2.11 below where the leaching rate is plotted against H_2SO_4 concentration. Gogoleva (2012) calculated the leaching rate by using initial rate method. The reaction order was determined to be about 0.69, which indicates a strong dependence of the rate on H_2SO_4 concentration.

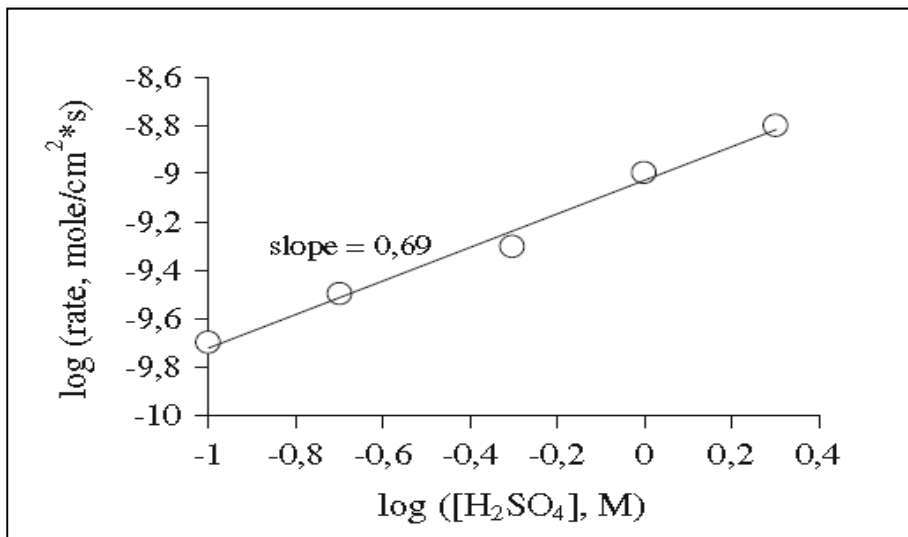


Figure 2. 11: The effect of H_2SO_4 concentration on the leaching rate of brannerite ore. Temperature: $70\ ^\circ C$; rotation stirrer speed: 500 rpm. Source: (Gogoleva, 2012)

Eligwe and Torma (1982) in their study of leaching of uranium ores² with the $\text{H}_2\text{O}_2 - \text{Na}_2\text{SO}_4 - \text{H}_2\text{SO}_4$ system also looked at the influence of pH on uranium yield. They found that increasing pH resulted in decreased uranium yield. They attributed the decrease in uranium yield to the deficiency in H^+ ion at high pH, which affects the oxidation of Fe(II) ion to Fe(III) ion which is responsible for the dissolution of the uranium(IV) present in the ore.

2.3.5 Effect of temperature on the reaction rate

The rate of dissolution of uranium increases as the temperature of leaching is increased (Gupta and Mukherjee, 1990). Increasing the temperature of the leaching operation reduces the reaction time required, thus increasing the capacity of the equipment and improving the extraction from refractory minerals (Merritt, 1971).

Tamrakar *et al.*, (2010) studied the effect that temperature has on uranium extraction. The effect was analysed at 50°C, 60°C and 70°C. They found that extraction dropped as the temperature decreased. Their findings are shown in figure 2.12.

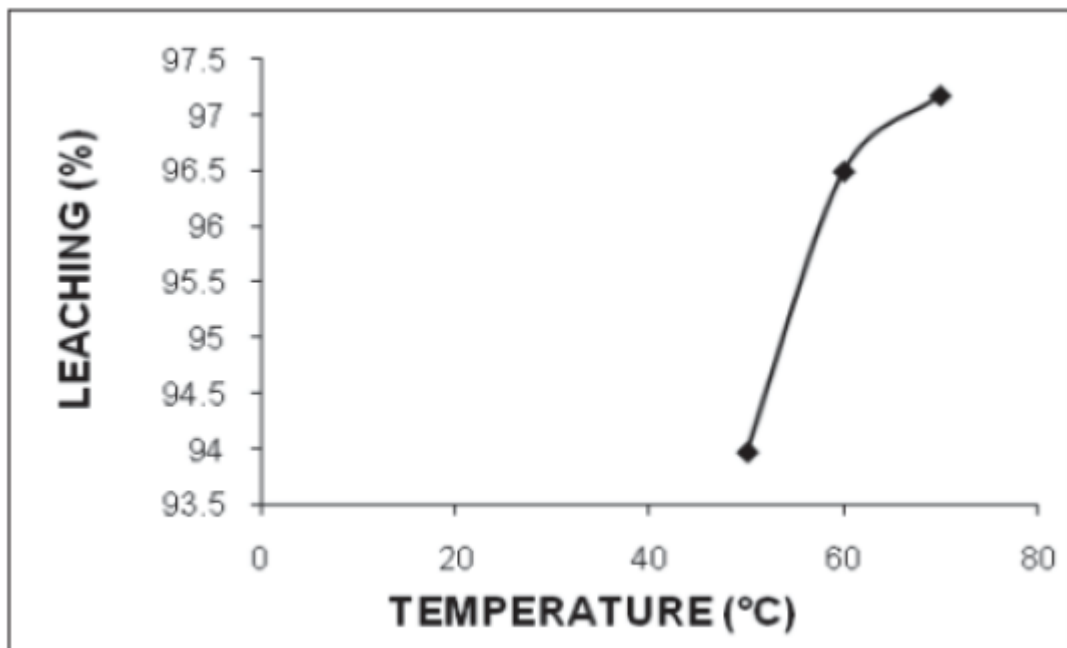


Figure 2. 12: Effect of temperature on uranium extraction. Source: (Tamrakar *et al.*, 2010)

² The authors did not mention the ore types but only referred to ores as sample A, B and C.

Even though temperature increases the leaching rate, it also increases the reagent consumption, the dissolution of other minerals besides those of uranium, and corrosion of equipment and vessels (Tamrakar *et al.*, 2010).

2.4 Modelling of the leach kinetics

The requirement for a good engineering model is that it must be the closest representation of reality which can be treated without too many mathematical complexities (Levenspiel, 1999). This means that the model should be simple, relevant to the process and easy to use.

2.4.1 Progressive conversion and shrinking particle models

In heterogeneous liquid-solid reactions there are a number of ways in which reactions occur at the particle surface (Othusitse and Muzenda, 2015). Levenspiel (1999) reports that the two commonly used models for modeling the kinetics of the reactions occurring at the particle surface are the progressive-conversion model and the shrinking core model. The progressive-conversion model (PCM) involves the continuous and progressive conversion of the solid reactant. In the shrinking-core model (SCM), various scenarios may exist (Othusitse and Muzenda, 2015);

- a) where the particle shrinks until it disappears as the reaction progresses; the shrinking particle model,
- b) the solid may react to produce an insoluble product³ whereby the reacting core shrinks while the particle does not change in size; shrinking core-unchanging size particle model and,
- c) the solid reacts and a gelatinous layer forms around the surface of the particle while the unreacted core shrinks; shrinking core-shrinking particle.

In hydrometallurgy the shrinking-core models are generally applied to describe the shrinkage of ore particles during mineral leaching reactions, which are a central unit operation in the hydrometallurgical ores treatment (Szubert, *et al.*, 2006). Evidence from a wide variety of

³ As the reaction moves into the solid, it leaves behind completely converted material and inert solid. They are referred to as "ash."

situations indicates that in most cases the shrinking-core model (SCM) approximates real particles more closely than does the progressive conversion model (PCM) (Levenspiel, 1999). Therefore the developed kinetics equations are based on the SCM.

For a chemically controlled reaction, the progress of the reaction is unaffected by the presence of any ash layer; the rate is proportional to the available surface of unreacted core (Levenspiel, 1999). This means that the surface concentration of the solid is constant because the new surface is exposed as the reaction on the surface takes place. The implication is that both the particles of unchanging size and the shrinking spherical particles can be modeled by the same equation. Levenspiel (1999) reported the decrease in radius or increase in fractional conversion of the particle in terms of τ , as at time t ,

$$\frac{t}{\tau} = 1 - \frac{r_c}{R} = 1 - (1 - X_B)^{1/3} \quad (2.24)$$

where τ is time for complete conversion of a particle, R is the initial radius of the particle, X_B fractional conversion and r_c is the radius of the core at time t .

Equation 2.24 applies to both the spherical particles of unchanging size and the shrinking spherical particles. However, the models for control by diffusion through a gas film differ for spherical particles of unchanging size and the shrinking spherical particles and are discussed below.

Shrinking-core model for spherical particles of unchanging size

Levenspiel (1999) reports that whenever the resistance of the gas film controls, the driving force is constant at all times during reaction of the particle. The equation for film diffusion control

$$\frac{t}{\tau} = 1 - \left(\frac{r_c}{R}\right)^3 = X_B \quad (2.25)$$

If the process is controlled by “ash diffusion” Levenspiel (1999) gave the following equation (2.26) to represent the behavior. Levenspiel (1999) considers mainly solid/gas systems where the use of the steady-state assumption allows great simplification in the mathematics.

$$\frac{t}{\tau} = 1 - 3(1 - X_B)^{2/3} + 2(1 - X_B) \quad (2.26)$$

Shrinking spherical particles

Levenspiel (1999) considers the reaction for particles to consist of three steps occurring in succession. The first step involves the diffusion of reactants from the main body of a bulk solution through the solution film to the surface of the solid. The second step has to do with the reaction on the surface between the reactant and the solid. The third and final step is the diffusion of reaction products from the surface of the solid through the solution film, back into the main body of the bulk solution.

For a film diffusion controlled reaction, the film resistance at the surface of a particle is dependent on numerous factors, such as the relative velocity between particle and fluid, size of particle, and fluid properties (Levenspiel, 1999). The equation for film diffusion control

$$\frac{t}{\tau} = 1 - \left(\frac{R}{R_0}\right)^2 = 1 - (1 - X_B)^{2/3} \quad (2.27)$$

The slowest step would be the rate controlling step of the reaction. When the reaction is chemically controlled (step two), Levenspiel (1999) reported that the behavior is identical to that of particles of unchanging size; and can be represented by Equation 2.24.

However, there are limitations associated with the models. The assumptions of this model may not match reality precisely. For example, the reaction may occur along a diffuse front rather than along a sharp interface between ash and fresh solid, thus giving a behavior between the shrinking core and the continuous reaction models (Levenspiel, 1999). Despite these limitations, Levenspiel (1999) states that these models are simple and can best represent the majority of reacting gas/liquid-solid systems.

The kinetics and rate-controlling steps of a fluid-solid reaction are deduced by noting how the progressive conversion of particles is influenced by particle size and operating temperature (Levenspiel, 1999). Crundwell (2013) reported that the rate of dissolution of leaching reactions is influenced by the concentration of reagents in solution and the temperature. The temperature dependence is often modelled by the Arrhenius equation,

$$K = Ae^{\frac{-E_a}{RT}} \quad (2.28)$$

where E_a is the activation energy for the reaction, and A is a constant known as the pre-exponential factor, R the gas constant and T the temperature.

An experiment where temperature is varied can distinguish between a chemically controlled or diffusion controlled rate. Generally, the activation energy is below 20kJ/mol for diffusion-controlled reactions in the aqueous phase, and it is above 40kJ/mol for chemical-controlled reactions (Crundwell, 2013).

Gogoleva (2012) reported that for temperatures varying from 35 to 90°C the dissolution reaction of brannerite was not controlled by the chemical reaction taking place on the surface of the mineral. The chemically controlled reaction is much more sensitive to the change in temperature than the diffusion controlled reaction. When Gogoleva (2012) plotted the function $[1 + 2(1 - a) - 3(1 - a)^{2/3}]$ versus time at the leaching temperatures varying from 35 to 90°C, he found that the dissolution rates of brannerite gave a good correlation with the model for ash diffusion control. These results are shown in figure 2.13.

In this case, two diffusion processes are supposed to compete in determining the reaction rate: diffusion of H^+ (from H_2SO_4) and diffusion of $Fe(III)$ ion through the TiO_2 layer produced by the surface chemical reaction upon the unreacted core (Gogoleva, 2012). The H^+ ion has a higher diffusion coefficient and therefore diffuses faster than $Fe(III)$ ion, so H^+ diffusion cannot be rate controlling. According to the above argument, one may be led to conclude that the diffusion of $Fe(III)$ ion through the TiO_2 controls the reaction rate. However, a possibility that the reaction rate can be controlled by the diffusion of uranium away from the reaction front may exist and therefore should not be ruled out.

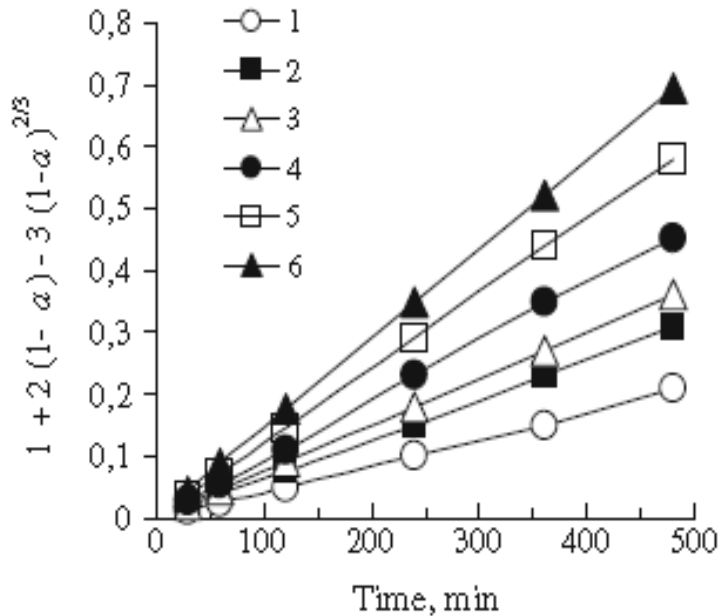


Figure 2. 13: Plots of $1 + 2(1 - a) - 3(1 - a)^{2/3}$ versus time for uranium dissolution at various temperatures, _C: 35 (1), 50 (2), 60 (3), 70 (4), 80 (5), 90 (6) source: (Gogoleva, 2012)

2.4.2 Modelling batch reactor kinetic data

A rate equation characterizes the rate of reaction, and its form may either be suggested by theoretical considerations or simply be the result of an empirical curve-fitting procedure (Levenspiel, 1999). One way of following the rate of reaction can be by following the concentration of the metal of interest in the ore during leaching. This can be done by taking samples at designated times and measure the concentration of metal of interest. The data generated this way is always related to time and is referred to as kinetic data. This allows one to plot curves of concentration versus time.

Newton (1975) studied the U(IV)- Fe(III) reaction in aqueous solution and reported that data generated were in accord with the integrated form of the second-order rate law:

$$Rate = -\frac{d[U]}{dt} = k[UO_2]^m[Fe(III)]^n \quad (2.29)$$

where k is the rate constant, m and n are the order of the reaction.

This rate law was further tested by varying the initial concentrations of Fe(III) in the range 1.2 to 5.2×10^{-5} M and U(IV) in the range 1.7 to 3.6×10^{-5} M. Over this range of concentrations,

Newton (1975) reported that the experimental values of k agreed with the average with a mean deviation of only 5%. Equation 2.29 shows that the rate-determining step involves a reaction between one U(IV) and one Fe(III) to give the intermediate U(V) or possibly a binuclear complex such as $\text{Fe} \cdot \text{UO}_2^{3+}$.

In an experiment where Fe(III) is kept constant, 2.29 is simplified to

$$\text{Rate} = -\frac{d[\text{UO}_2]}{dt} = k[\text{UO}_2]^m \quad (2.30)$$

In logarithmic form, 2.30 becomes

$$\ln \frac{d[\text{UO}_2]}{dt} = \ln k + m \ln[\text{UO}_2] \quad (2.31)$$

Hence, we obtain the order m , of the reaction from the slope of the plot of \log rate vs \log $[\text{UO}_2]$. The rate of the reaction can be seen to be dependent on the surface area of UO_2 which suggests that the rate will decrease as uranium surface area decreases.

Levenspiel (1999) identified two methods of analysing kinetic data, which are the integral and the differential methods. In the integral method of analysis we guess a particular form of rate equation and, after appropriate integration and mathematical manipulation, predict that the plot of a certain concentration function versus time should yield a straight line (Levenspiel, 1999).

The integrated rate laws are summarised below.

Zeroth order integrated rate law: $[\text{A}] = [\text{A}]_0 - kt$
A plot of $[\text{A}]$ vs t will be linear, with a slope of $-k$.

First order integrated rate law: $\ln[\text{A}] = \ln[\text{A}]_0 - kt$
A plot of $\ln[\text{A}]$ vs t will be linear with a slope of $-k$.

Second order integrated rate law: $\frac{1}{[\text{A}]} = \frac{1}{[\text{A}]_0} + 2kt$
A plot of $\frac{1}{[\text{A}]}$ vs t will be linear with a slope of $2k$.

The rate law that fits the data satisfactorily (yielding a straight line) becomes the rate equation. The slope will be equal to bk , where k is the rate constant and b is -1 for zeroth and first order integrated law and 2 for second order integrated law.

The knowledge of the order of reaction gives information on the reaction mechanism, and may help to identify the rate-determining step. Added to this, the order of a reaction gives information on the relationship between concentration and rate. They are often positive integers, but they may also be zero, fractional, or negative. Reaction orders can be determined only by experiment.

The differential method however, does not require the integration of mathematical equations but rather fitting the rate equations to the data. Levenspiel (1999) discusses the limitations of both methods. The integral method can only test for a particular mechanism or rate form; the differential method can be used to develop or build up a rate equation to fit the data.

2.4.3 Multiple regression models

A mathematical expression such as $Y=f(X)$ may be used to model kinetic leach data. Where Y , the effect of interest is the response and X the cause is the variable. Multiple Regression analyses the relationship between one dependent variable (Y) and multiple independent variables (X 's) (SigmaXL, 2014). The empirical equation that is generated is of the form:

$$Y = b_0 + b_1 \cdot X_1 + b_2 \cdot X_2 + \dots + b_n \cdot X_n \quad (2.32)$$

Where Y is the response or leach rate in this case, b_i are the coefficients and constant terms generated by the least square method and X_i are the input variables. The model should consist of only the variables that have an effect on the response. Regression analysis which often results in a model when used, can determine parameters of empirical mathematical models. The essence of the method is to minimise the sum of squared residuals (*Milivojevic et al., 2012*). This is achieved by fitting the plane that comes as close to the observations as possible. In other words, one wants the values of b_i that minimize the sum of squared errors.

This approach combined with design of experiment (DOE) in conjunction with the response surface method (RSM), together with the two-level and four-factor full factorial central composite design (CCD) plan, were used by *Milivojevic et al., (2012)* to model the leaching kinetics of a complex nickel ore.

2.4.4 Exponential empirical models

Exponential empirical models on the other hand, are models that are generated by fitting the curve to the kinetic data. Software packages that can be used to fit equations to the curves generated from experimental data are available. One of such packages is CurveExpert Professional 2.0.2. This software produces possible models arranged according to the increasing coefficient of determination usually denoted by R^2 . The closer R^2 is to 1, the better the model would fit the experimental data.

The shortcoming associated with these kinds of models is that they can only accommodate one variable at a time. One needs to keep other parameters constant and only evaluate the effect of a single factor. The equation generated is often based on the curve obtained with a fixed set of parameters, in the case where a parameter has been altered; a new curve obtained would not fit the condition anymore.

2.5 Conclusions and research direction

The literature review has shown that there exist factors that influence the leaching kinetics of uranium that if well controlled, better extraction can be achieved at Rössing Uranium Ltd. Some of these factors like the pH are ore specific. It has also been shown that the conditions in which the leaching is done have an influence on the leach kinetics. This research therefore, as outlined in the introduction, aims to establish the effects that pH, total iron and ORP have on Rössing Uranium ore, which contains mainly uraninite as uranium bearing mineral. To this end, it also aims to come up with a model that can predict leach rate, given the different conditions which can be used to optimise the process. This model should allow for more refining as more plant data become available. In addition, the model should have the ability to be used as an online tool available to metallurgists.

2.6 Summary

The majority of the work reviewed here looked at the influence that pH, pulp density, ORP, total iron and temperature have on brannerite and uraninite dissolution. It emerged that these factors have a significant influence on the dissolution of uraninite/brannerite, though there are some contradictions in literature as to the extent of the influence. As a result the outcome highlighted the fact that each ore is unique, and therefore the parameters have to be optimised for specific ores.

Table 2. 1: Summary of previous research on Uranium dissolution rates.

Parameter	Uranium dissolution
Pulp	Lower pulp density yields good dissolution rates
ORP	Increasing ORP results in increased dissolution rate. However, high ORP does not necessarily imply high dissolution rates.
Iron concentration	Increasing iron concentration for ORP values of 460 – 500mV vs Ag/AgCl results in increased dissolution rates.
pH	Decreasing the pH generally results in increased dissolution rates.
Temperature	Increase in temperature increases the dissolution rates.

Chapter 3: Leaching method verification

This chapter presents the work done in verifying the leach method used to generate the kinetic data. It shows how the two-leach method employed in the study of uranium kinetics was arrived at.

3.1 Background

Laboratory equipment and systems may have a big influence on the outcome of the experimental results. It was against this background that a decision was taken to verify the leach method and systems before the experimental leach investigations could start. This involved conducting a series of leach experiments under the same conditions to gain a good understanding of:

- the total error associated with the extraction determined from ‘best-practice’ leach tests;
- the relative magnitudes of sub-sampling (from vessel and final residue), analytical and leach control error that contribute to the total extraction error;
- the best method that could reduce the overall error.

Once the above was established, test work to investigate the uranium leach kinetics could be carried out reliably. The target for the experimental work was to have a maximum of 0.5% (95% confidence interval) difference in extraction between leach tests. This would give confidence in the results that would be obtained during the uranium leach investigation.

3.2 Method

The agitated leach tests were conducted on a leach feed sample which was blended at Mintek in Johannesburg, South Africa. A 2.5kg ore sample was used per leach. Table 3.1 shows the conditions used for the verification leach. These leach tests were repeated several times under the same conditions.

Table 3. 1: Conditions used in the verification leach

Parameter	Values
pH	1.6
ORP (mV) ⁴	525
Temp (°C)	35
Agitation Speed (rpm)	450
Solids % (%w/w)	70
Fe Concentration (M)	0.085
Mass of ore (kg)	2.5
PSD _(d80) (microns)	1000
Volume of pulp (l)	2
Size of sub-samples (g)	250

The leach tests were carried out in the reactor shown in figure 3.1. The reactor had an inside diameter of 12 cm and 27 cm length. The required amount of return dam solution (RDS) was first added to the reactor and pre conditioned to 29°C. Thereafter, a 2.5kg ore sample was slowly introduced to the reactor while stirring to avoid the solids settling at the bottom of the tank. The set temperature of 35°C was achieved due to an exothermic reaction after the addition of 98% (wt %) concentrated sulfuric acid to the slurry.

The RDS used for the leach contained the required iron concentration. The oxidation - reduction potential and the pH were maintained by the automated addition of 10% sodium permanganate solution and sulfuric acid respectively. The total iron concentration and ORP in the slurry were controlled at the values shown in the table 3.1. ORP was measured using a silver/silver chloride electrode. The online pH and ORP readings were verified with a hand held meter during the leach and adjustments (calibrations) of the probes were done when necessary.

⁴ Measured relative to a Ag/AgCl electrode filled with 3 M KCl.



Figure 3. 1: Shows the leach reactor and baffles in leach reactor



Figure 3. 2: The Impeller used for stirring in the reactor

Slurry samples of about 200g were taken using a sampler shown in figure 3.3 at 2, 4, 6, 9 and 11 hours of leach. The samples were then split into two 250 ml centrifuge bottles and placed into the centrifuge. The solution was titrated to determine the concentration of H_2SO_4 , Fe(III) and Fe(II) in the leach reactor. The solids were washed with pH 2 water and put in the oven at $210^{\circ}C$. The tube⁵ used for sub-sampling from the reactor is shown in figure 3.3.

⁵ The tube was inserted in the reactor with the plug open. Once the slurry had entered the tube, the plunger was pulled and hence trapping the slurry in the tube. The tube was inserted carefully to avoid the impeller in the reactor.



Figure 3. 3: The sampling device used to sub-sample from the vessel during leaching

The final residue was pulverised prior to splitting out a sub-sample for assay. Work done by Sillilo (2012)⁶ where subsampling error associated with pulverised and non-pulverised residue were compared suggested that the subsampling error for pulverised was lower than the non-pulverised residue. This was the reason why the final residue was pulverised prior to splitting out a subsample for assay.

The samples collected from the leaches were sent to Bureau Veritas Mineral Laboratories (BV) located in Swakopmund and Rössing Uranium Ltd laboratories (RUL) for assaying. Results from BV were used for reporting while RUL's results served as a check only. Errors were determined on the % extraction. The uranium in the sample was determined by Inductively Coupled Plasma Mass Spectroscopy (ICP – MS). An ICP-MS combines a high-temperature ICP (Inductively Coupled Plasma) source with a mass spectrometer. The ICP source converts the atoms of the elements in the sample to ion. These ion are then separated and detected by the mass spectrometer (Wolf, 2005). The results were reported as UO₂ in kg/t.

3.3 Results and discussion

3.3.1 Analytical error

Total analytical error has been a useful metric both to assess laboratory assay quality and to set goals (Krouwer, 2002). The error was determined based on the variation between the sets of triplicate or 5 repeat assays. This error made up part of the sub-sampling and overall error. The reference material analysed in the same run was found to be within the expected range.

For the 5 repeats, the standard error achieved was 0.08%, an apparent improvement compared to triplicate assays which was 0.11% (see appendix A). This difference was due to

⁶ As part of the method validation, a comparison between an error associated with sampling from pulverised residue and non-pulverised residue was done.

the number of repeat assays per sample. More repeats reduced the analytical error as it was demonstrated. This error made a relatively small contribution to the overall error.

3.3.2 Sub-sampling error

Two types of sub-samples were taken in the leach test, sub-sampling from the vessel during leaching at designated times, and sub-sampling from the final residue.

a) Sub-sampling error from the vessel

This error was determined by taking repeat sub-samples from the vessel during the leach using the sampling tube (figure 3.3). The 95% confidence interval achieved was 1.74%. This value was very high, and reliance on this type of sample could not enable the achievement of the target confidence interval for predicted extraction. As a result, the kinetic data generated using this method could not be trusted. There was a need to find a better method that could generate dependable intermediate data points.

b) Sub-sampling from the final residue

This error was determined by sampling the final leach residue repeatedly and assaying each sub-sample five times. The 95% confidence interval achieved on residue was 0.65% compared to 1.74%, achieved on sub-sampling from the vessel during the leach. This result did show that data points obtained from the entire residue would be more reliable.

3.3.3 Overall test error

The overall variation between tests was determined by comparing the extractions of different “identical” tests. The overall error included analytical and sub-sampling errors, but also variations in leach control.

Given the better results (compared to in-situ) found in sub-sampling the entire residue, it was decided to conduct several two-leach tests where one ended at 7 hours of leaching time and the other at 13 hours, whose data could be combined to form one extraction curve. This was thought to give at least one reliable intermediate data point. The results are shown in figure 3.4.

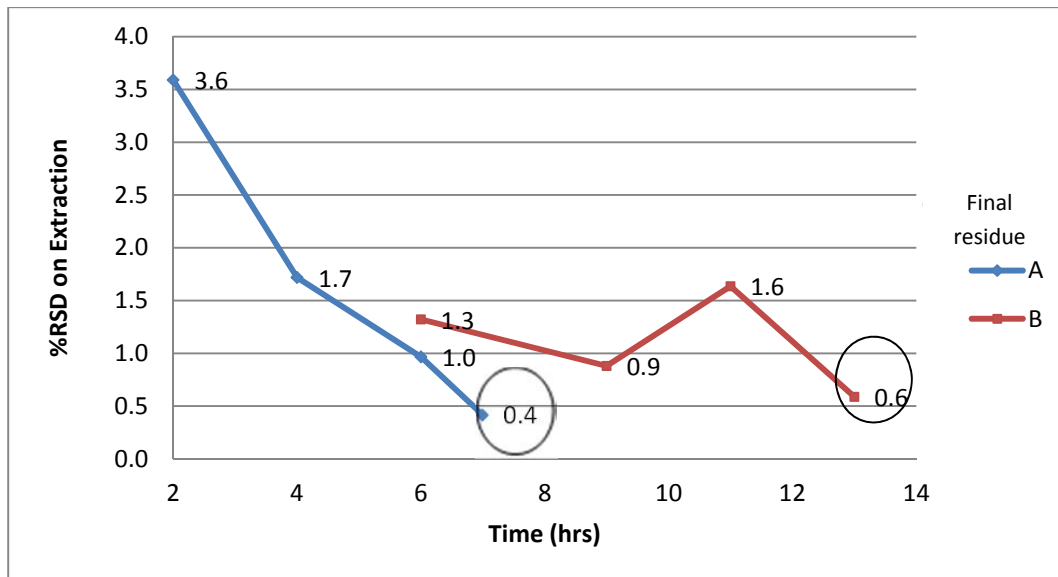


Figure 3. 4: Overall extraction error at each sample time

Figure 3.4 shows how overall extraction error at each sample time was highly impacted by sub-sampling error. ‘A’ in the graph represents the leach that was stopped after 7 hours and ‘B’ stopped after 13 hours of leaching. In both leaches, the sampling error related to the final residues was lower as compared to the in-situ vessel sampling, at 0.4 - 0.6% compared to 0.9-3.6% for vessel subsamples. The errors of all the sampling times (from the vessel during the leach) were all above the targeted error of 0.5%.

Stopping a leach after 7 hours of leaching allowed one to get a more reliable intermediate data point for the overall extraction curve. This resulted in the method termed, the two-leach method.

The graph also shows that the early data points have the greater error, which is likely to be due to the fact that the highest proportion of the leaching occurs in the early part of the test.

Figure 3.5 below is a stacked column graph showing how overall error is made of the analytical error, sub-sampling error and “other” error (e.g. Leach control). Sub-sampling error makes the biggest contribution to the overall error as is shown below. The sub-sampling error is so much larger for vessel sub-sampling compared to residue sub-sampling error.

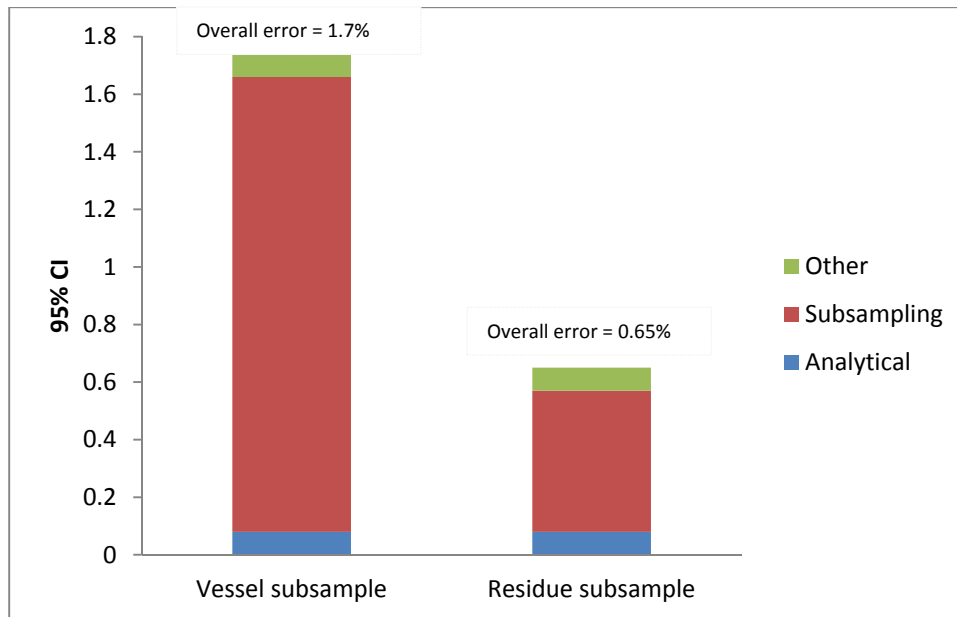


Figure 3. 5: Contributions to the overall error

3.4 Conclusion and recommendations

The data showed that the sub-sampling error was the biggest error of them all and still remained above 0.5% even when the analytical error (which forms part of it) was subtracted.

- **Overall test error:** The predicted extraction had a 95% confidence interval of 0.66%, which is 0.16% higher than the targeted 0.5%. The main contributor to this was determined to be the sub-sampling error.
- **Sub-sampling error:** Sub-sampling from the vessel resulted in a high sub-sampling error. A 95% confidence interval of 1.74% was the best achieved value, though it has varied in different trials.

The sampling error achieved on the final residue has a 95% confidence interval of 0.65%, much better than for vessel sub-sampling.

A 7 hour final residue has given a more reliable intermediate data point, rather than relying on vessel sub-sample data alone. This was made possible by the two-leach method.

- **Analytical error:** The error was reduced by increasing the number of assays from three times, that gave 0.11% to assaying five times which gave 0.08%.

- **Other error:** This error appears not to have a great impact on the overall test error with the majority contribution coming from the sub-sampling error.

The following was recommended for going forward:

- Based on the results, it was possible to perform investigative leach tests where parameters could be varied in that leach laboratory using the two-leach method.
- It was also recommended that a reliable quality control procedure be in place to continuously monitor the performance of the laboratory during the leach investigations test work.

Chapter 4: Materials and methods

This chapter details the collection, handling and the preparation of the bulk samples used in the leach tests. The set-up of the equipment and the reagents used in the test work are also explained in this chapter. It further looks at the method employed to generate results.

4.1 Bulk sample collection and blending

Two bulk samples (bulk 1 and 2) were collected periodically from the Rössing Uranium plant. They were collected from the rod mill discharge over a period of two months. After collection, they were washed with pH 2 water to remove dissolved uranium and then placed in the oven to dry over night at 210⁰C. Once dried, the samples were rolled to break lumps and stored in plastic bags. During the period of sample collection, the processing plant may have been supplied with ore with different constituents e.g. grade. This was the reason why the sample was blended.

Bulk 1 was blended at Mintek and was used for leach method verification work and quality control leaches during the investigations of leach kinetics test work. Bulk 2 was homogenised in-house and was used for the leach kinetics investigations test work. Both bulk samples were sampled at random and the blending met the set requirements (Rössing, 2012). The bulk samples were characterised and the information is summarised in the table below.

Table 4. 1: Bulk sample characterisation

Bulk sample	UO ₂ Grade (kg/t)	Calc index (kg/t)	% CGS	d ₈₀ (µm)
Bulk 1	0.322	9.1	2.6	1000
Bulk 2	0.207	8.1	3.2	800

The calc index (CI) is the measure of the acid consuming properties of the ore while %CGS is the percentage cordierite Gneiss schist present in the ore. The CI was determined by exposing a sample of ore to concentrated sulfuric acid for a given period of time, after which the amount of acid consumed was determined (the difference in concentration between the initial and final). The CI and CGS are important because they affect pH and oxidation reduction-potential

control during the leach. Figure 4.1 below shows the mineral liberation analyser (MLA) results of the bulk sample. It shows that uraninite occurs as relatively large anhedral particles with a high degree of liberation in the size range <100µm (Ryan, 2011).

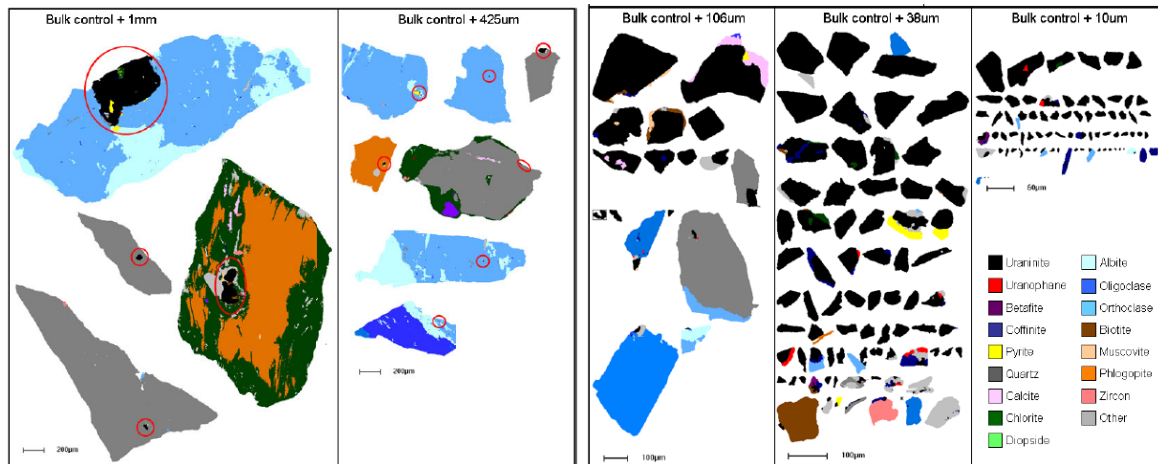


Figure 4.1: MLA particle images of uraninite (circled and in black) in the bulk control. Source: (Ryan, 2011)

4.2 Reagents

A synthetic acidic solution that contained ion as would characteristically be found in the recycled process solution from the plant was used as the start-up solution. The typical concentrations of the recycled process solution are shown in table 4.2. The required ferric/ferrous solution was only added to the vessel when the pH was below 2. This was done to avoid ferric hydrolysing at pH above 2. A 98% (wt %) concentrated sulfuric acid (H_2SO_4) and 10% sodium permanganate ($NaMnO_4$) solution were added into the leach vessel during the leach to maintain the pH and ORP respectively. It was easier to use $NaMnO_4$ (solution) in the laboratory as compared to MnO_2 (powder) which is used on the plant due to the solubility of MnO_2 , which might have been a challenge in the laboratory leach vessels. MnO_2 takes a while to dissolve and therefore would have resulted in difficulties to maintain or attain the targeted ORP. Added to that, the dosing mechanism of the equipment used was designed for solutions. The consumption of $NaMnO_4$ was converted to MnO_2 consumption.

Table 4. 2: Typical composition of recycled process solution

	Units	Plant Solution Average	Synthetic Solution
Mg	g/L	2.12	2.12
Mn	g/L	2.26	2.30
Na	g/L	1.91	1.90
Al	g/L	0.72	0.72
K	g/L	0.22	0.25
Ca	g/L	0.62	0.40
NO₃⁻	g/L	0.084	0.080
Cl⁻	g/L	1.51	1.50
SO₄²⁻	g/L	21.23	29.58
H₂SO₄	g/L	1.22	0.98
pH	-	1.91	2

4.3 Iron dissolution tests

The bulk samples used in this study were subjected to iron dissolution tests. These tests were done to establish the natural ORP and iron content in the ore. This involved leaching the ore for 2.5 hours under the following conditions; 35⁰C, pH of 1.6 and no oxidant was added. The solution from the leach residue was filtered and titrated for Fe(III) and Fe(II) and the ORP was measured during the leach. The results from these tests were used to determine the concentration of Fe(III)/Fe(II) in the start-up solution. The table below shows the results for bulk 2 (ore used in the test work). The starting iron concentrations were adjusted to take into account the amount of iron which would be leached from the ore at each pulp density. Studies done by Siliilo (2012) on this ore have shown that more than 90% of iron present in the ore was leached within the first 2.5 hours.

Table 4. 3: Dissolution test results

Sample	Ferric (M)	Ferrous (M)	Natural ORP (mV) vs Ag/AgCl
Bulk 2	0.028	0.015	440

As can be seen in the table above, more than 60% of iron was found as ferric. The reported iron could not have come from comminution as the ore was washed with pH 2 water before the dissolution test. The studies done by Ryan (2011) show that the gangue minerals associated with this ore contained significant amount of iron at least 10% by weight. This restricted the test work to 440 mV vs Ag/AgCl as the lowest ORP value to be considered in this test work.

4.4 The two-leach method

The two-leach method (explained in section 3.3.3) was used. A mass of 2.5 kg of ore was leached in each of the stirred vessels, which were immersed in a water bath. Acid and oxidant addition were done automatically using a Metrohm model 902 titrator controlled by the tiamo™ software. The temperature of the water bath was controlled by a heater equipped with a thermostat. The tiamo™ software made it possible to maintain the required set points (ORP and pH) for the different parameters. The set-up is shown below.

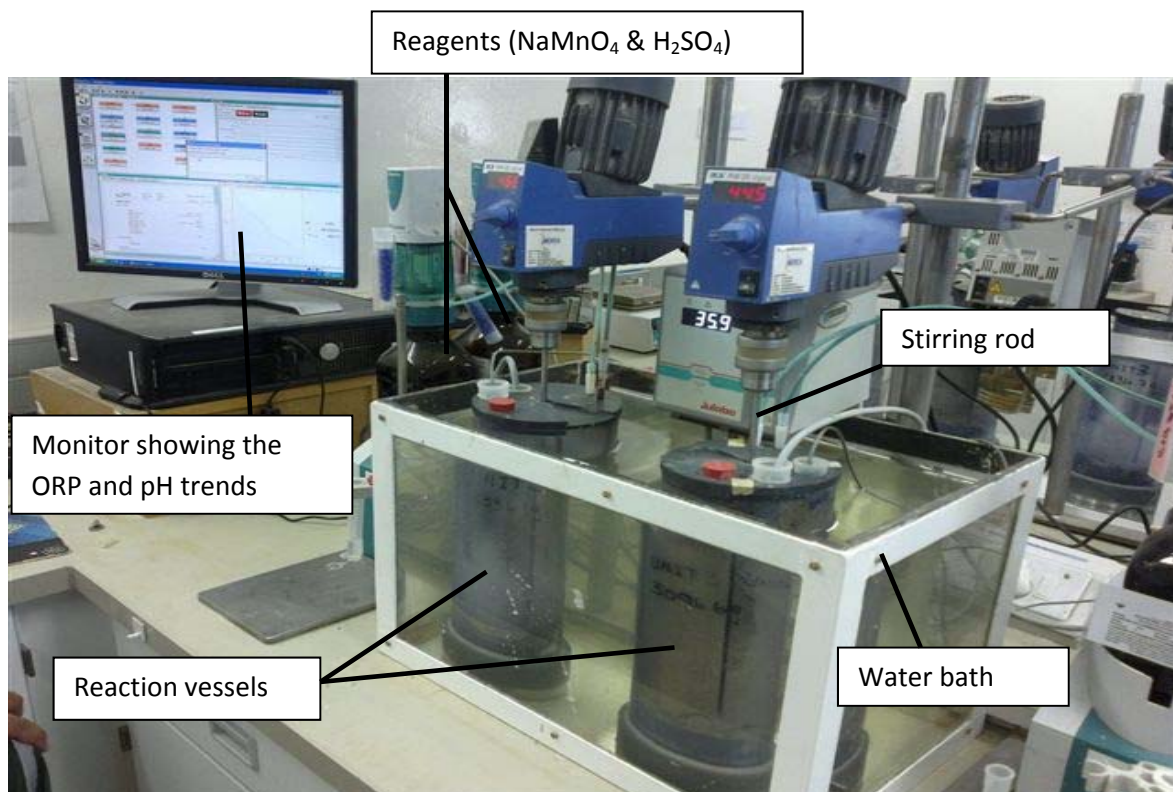


Figure 4. 2: The experimental set-up showing the leach vessels in the water bath

The ORP electrode used was the Combined LL Platinum containing 3M KCl solution supplied by Metrohm. The pH Probes (Metrohm Unitrode with Pt1000 temperature sensor) was also

supplied by Metrohm. All potential values are reported using a standard silver/silver-chloride electrode (SSCE).



Figure 4. 3: The ORP probe and the probe guard

Sub-samples were taken after every two hours during the leach. The residue and intermediate sub-samples were washed with pH 2 water and allowed to dry overnight at 210⁰C. The entire residue was then pulverised before it was sub-sampled for analysis. The samples were sent to Bureau Veritas Mineral laboratory located in Swakopmund for analysis. At BV laboratories, the samples were fused with sodium peroxide and subsequently the melt was dissolved in dilute hydrochloric acid for analysis. The uranium in the sample was determined as explained in section 3.2 above.

Chapter 5: Results and Discussion

In this chapter, results from the test work are presented and discussed. Parameters such as the ORP, iron concentration, and pH were varied to help understand the effect they have on the extraction and leaching kinetics of uranium. In addition, these three factors were also looked at using the full factorial experimental design at two levels. This approach helps to elucidate the main effects and how the parameter interactions impact on uranium extraction and the kinetics. The findings are discussed in the subheadings below. The samples from where the data were generated were taken and treated as described in chapter 4. Table 5.1 shows the test work layout.

Table 5. 1: Shows the tests conducted to generate the kinetic data

Number	Ore type	Total Fe (M)	ORP (mV) vs Ag/AgCl	pH	Temperature (°C)	% Solids
1	ROM	0.072	440	1.6	35	70
2	ROM	0.072	450	1.6	35	70
3	ROM	0.072	475	1.6	35	70
4	ROM	0.072	500	1.6	35	70
5	ROM	0.072	525	1.6	35	70
6	ROM	0.072	550	1.6	35	70
7	ROM	0.054	525	1.6	35	70
8	ROM	0.054	450	1.6	35	70
9	ROM	0.054	500	1.6	35	70
10	ROM	0.054	550	1.6	35	70
11	ROM	0.081	525	1.6	35	70
13	ROM	0.072	525	1.3	35	70
14	ROM	0.072	525	1.9	35	70
15	ROM	0.072	525	1.9	35	70
16	ROM	0.072	525	1.2	35	70
17	ROM	0.090	525	1.6	35	70
18	ROM	0.054	525	1.9	35	70
19	ROM	0.072	525	1.0	35	70

The following parameters were kept constant throughout the test work.

Table 5. 2: Conditions kept constant throughout the test work

Parameter	
Retention time	13 Hours
Stirring rate	470 rpm
Temperature	35 °C
Pulp density	70 %

5.1 The effects of parameters on uranium extraction

In order to understand how a specific parameter, namely ORP, iron concentration and pH affects extraction, each parameter was varied while others were kept constant. The two-leach method was used. Percentage extraction was calculated using equation 5.1.

$$\%E = \frac{U_0 - U_t}{U_0} \times 100 \quad (5.1)$$

Where U_0 is the uranium grade and U_t is uranium left after time t .

5.1.1 The effect of total Fe concentration on uranium extraction

To understand the effect total iron concentration has on uranium extraction, different iron concentrations were considered, namely, 0.054, 0.072, 0.081, 0.090 M. The other parameters such as the ORP = 525 mV vs Ag/AgCl and pH=1.6 were kept constant. The graph below shows how uranium final extraction was affected by the change in iron concentration.

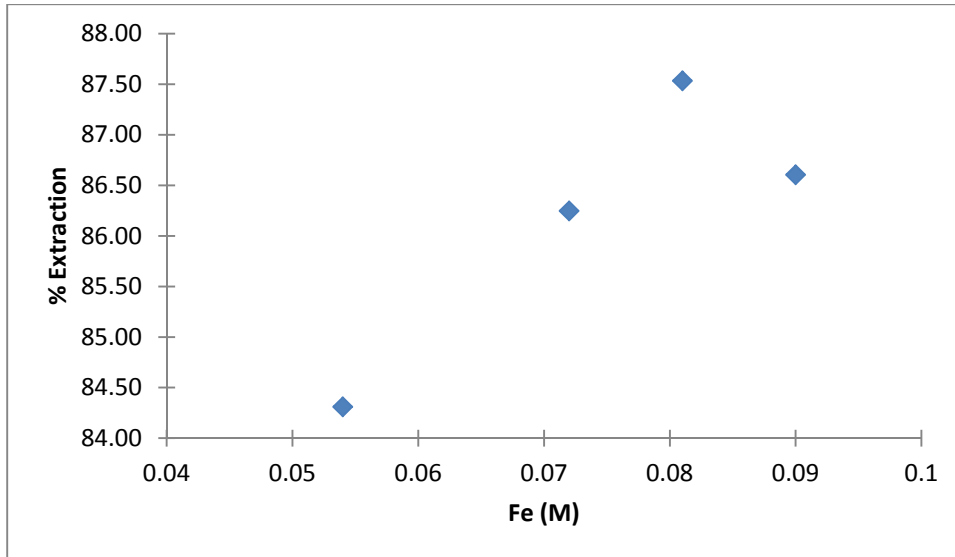


Figure 5. 1: The effect of iron concentration of uranium extraction

It can be observed from figure 5.1 that uranium extraction increased with the increase in total iron concentration. The ORP of 525mV at which these tests were conducted was found to have more than 91% of the total Fe as Fe(III) ion, see table 5.3. Fe(III) is the species required to oxidise primary uranium into secondary uranium as discussed in section 2.3.2. At 525mV, the increase of total Fe in the slurry equates to the increase in concentration of Fe(III) ion. This may explain the observed increase in uranium extraction as total Fe was increased. At total Fe concentration of 0.09M, extraction seems to have dropped, it is not clear why that would be the case. Work done by Gogoleva (2012) on brannerite ore found that the dissolution rate dropped above 0.1M concentration of Fe(III). It was proposed that it was due to the precipitation of hydrates such as $Fe_2O_3 \cdot H_2O$ on the surface of the ore. More work needs to be done to ascertain whether this could be the case with uraninite ore as well.

Table 5. 3: Shows the measured proportion of Fe(III)/Fe(II) from the Fe concentration of 0.068 M at different ORP values

ORP (mV)	440	450	475	500	525	550
Fe (III) (M)	0.030	0.036	0.047	0.057	0.062	0.064
Fe(II) (M)	0.038	0.032	0.021	0.011	0.0061	0.0043

From table 5.3, the proportion of Fe(III) can be seen to increase with the increasing ORP.

5.1.2 The effect of ORP on uranium extraction

In order to study the effect ORP on uranium extraction, different values of ORP were considered, namely, 440, 475, 500, 525 and 550mV vs Ag/AgCl. Iron concentration was kept constant at 0.072 M and pH at 1.6. The results are shown in the figure 5.2 below.

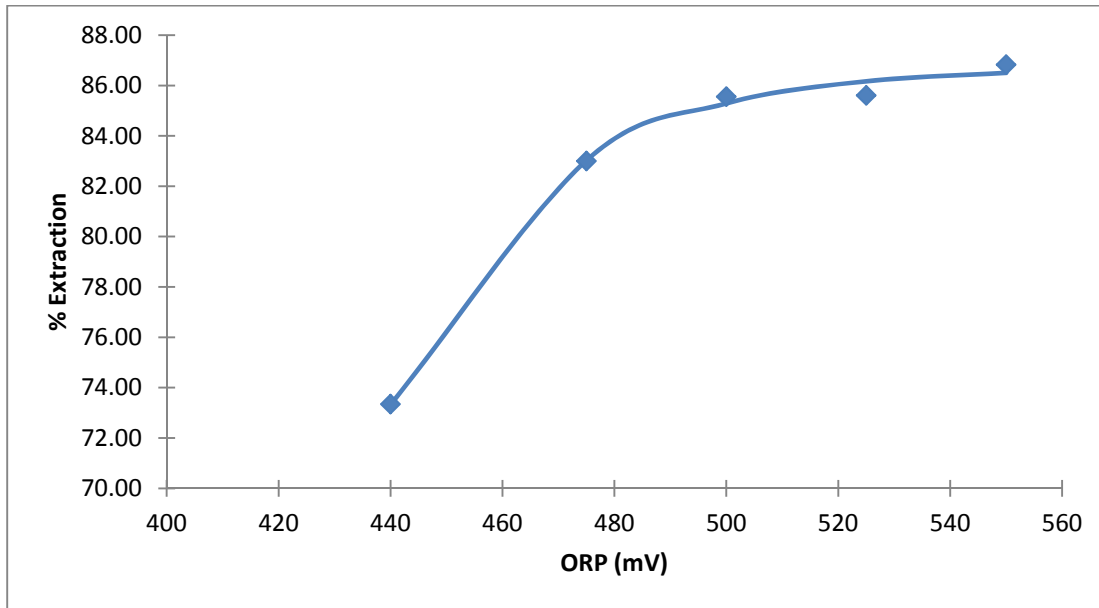


Figure 5. 2: The effect of ORP on uranium extraction

It can be observed that the extraction generally increases as ORP is increased. The increase in ORP equates to the increase in Fe(III) species in the slurry. As discussed in 5.1.1, increased concentration of Fe(III) ion results in increased uranium extraction. The graph shows that uranium extraction plateaus as from 500mV; this can be explained when one takes table 5.3 into account. Table 5.3 shows that above 500mV, more than 80% of the total Fe is present in the form of Fe(III). So the increase in ORP would not have a major impact on extraction as the majority of the total Fe is already in the Fe(III) state. Therefore increasing the ORP beyond 500mV does not improve the extraction significantly.

5.1.3 The effect of pH on uranium extraction

In this test, pH values were varied as 1.3, 1.6 and 1.9 to evaluate the effect pH has on uranium extraction. Parameters such as ORP = 525mV vs Ag/AgCl and iron concentration = 0.072M were kept constant. The results are shown in figure 5.3 below.

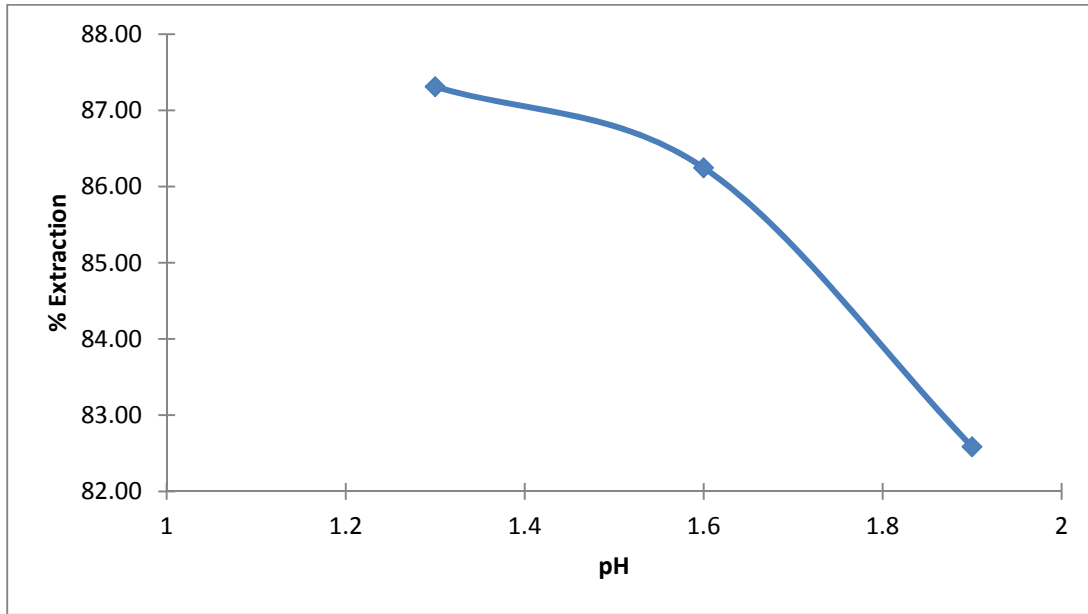


Figure 5. 3: The effect of pH on uranium extraction

It can be observed that as pH increases, uranium extraction decreases. This may be explained by the fact that Fe(III) ion responsible for oxidising uranium was found to precipitate at a pH just above 2 in this system. The other explanation may be that some dissolved uranium in the slurry may also start to precipitate at pH above 2 as was observed in the system.

5.2 The effect of parameters on the kinetics

The section above looked at how the parameters affect uranium extraction after 13 hours retention time. This section will focus on the effect of these parameters on the uranium leach kinetics. Iron concentration, ORP and pH were varied one at a time to help study the effect each has on the uranium leach kinetics.

Samples were taken at 2, 4, 6, 7, 9, 11 and 13hrs during the leach. The samples taken at the 7th and the 13th hours were taken from the residue. This was due to the findings discussed in

chapter 3. The samples were prepared and analysed as discussed in section 3.2. The kinetic data of uranium dissolution obtained from the test work were analysed using the differential method to ascertain the order of reaction. Once the order of reaction was established, the integral method was used to analyse the kinetic data to determine the effect the parameters have on uranium leach kinetics. Levenspiel (1999) observed that it is easy to use the integral method and is recommended when testing specific mechanisms, or when the data are so scattered that one cannot reliably find the derivatives needed in the differential method.

Using differential method to establish the order of the reaction

The differential method of analysis deals directly with the differential rate equation to be tested, evaluating all terms in the equation including the derivative dC_i/dt , and testing the goodness of fit of the equation with experiment (Levenspiel, 1999). The differential equation to be considered in this work is equation 2.31. Table 5.4 shows the kinetic data used to evaluate the derivative.

Table 5. 4: Kinetic data used to evaluate the derivative

Time (hrs)	U_i (mol/L)	$\ln U_i$	$-dU_i/dt$ ($Lmol^{-1}h^{-1}$)	$\ln (-dU_i/dt)$
0	0.00087	-7.05		
2	0.00027	-8.21	2.96E-04	-8.12
4	0.00019	-8.60	4.41E-05	-10.030
6	0.00016	-8.76	1.4E-05	-11.18
7	0.00015	-8.80	6.05E-06	-12.06
9	0.00014	-8.90	7.23E-06	-11.84
11	0.00012	-9.02	7.48E-06	-11.80
13	0.00011	-9.11	5.29E-06	-12.15

ORP =525mV (Ag/AgCl), Fe =0.072 M, pH =1.6. U_i is $[UO_2]$ in the solid. The units (mol/L) is the concentration of U if it were dissolved in solution.

The plot of $\ln (-dU_i/dt)$ vs $\ln [U_i]$ to determine the slope is shown in figure 5.4 below.

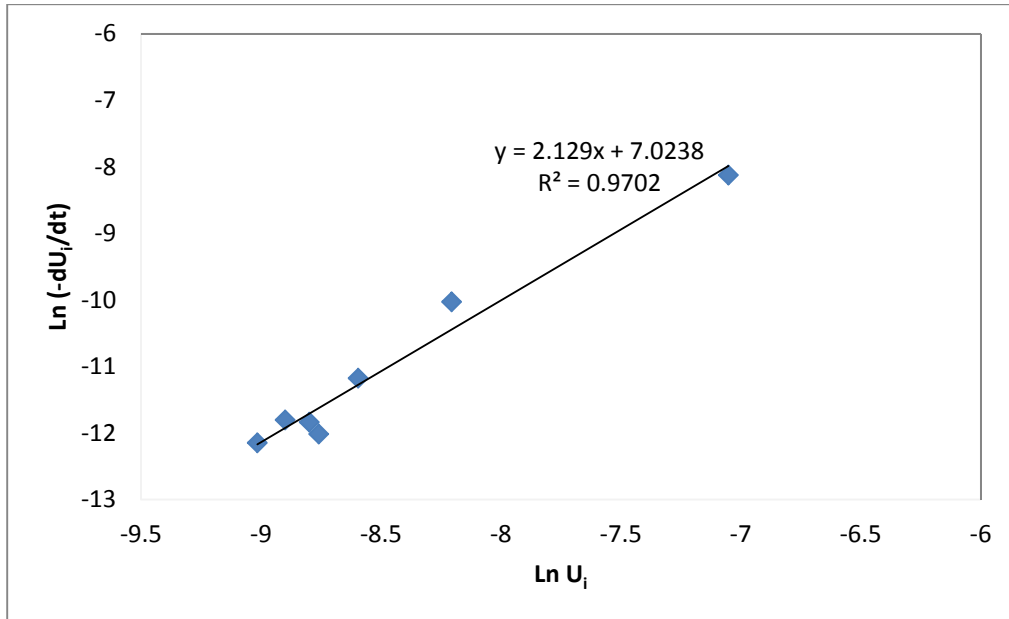


Figure 5. 4: Test for an nth-order rate form by the differential method.

From the figure 5.4, equation 2.31 becomes

$$\ln \frac{d[UO_2]}{dt} = \ln 7.02 + 2.13 \ln[UO_2] \quad (5.2)$$

From equation 5.2, one can see that $m=2.13$ which implies that the reaction is second order with respect to UO_2 . Newton (1975) also reported second order in UO_2 dissolution.

The effect of each parameter on the leach kinetics was determined by plotting the rate constants vs the corresponding change in the parameter. The rate constants were determined from the second order integrated rate law for each level of the parameter. The rate constant can allow conclusions to be made regarding the rate of a reaction. The higher rate constant values indicate the faster reaction rates.

5.2.1 The effect of Oxidation-Reduction Potential on leach kinetics

To understand the effect of Oxidation–Reduction Potential (ORP) on leach kinetics, six ORP values were considered, namely, 440, 450, 475, 500, 525 and 550 mV vs Ag/AgCl. Total iron concentration and pH were kept constant at 0.072M and 1.6 respectively. The lower bound was the lowest that could be achieved due to the inherent iron in the ore which was found to be mainly in the Fe(III) ion state. The initial/natural ORP before the oxidant was added was

about 440 mV. These leaches were conducted under the same conditions, only varying the ORP. The desired ORP was maintained by the addition of 10% NaMnO₄ solution.

The integral method was used to analyse the data. The second order integrated rate law yielded a straight line when $\frac{1}{[UO_2(t)]}$ (the inverse of UO₂ concentration left in the solid phase after leaching time, t) was plotted against time in hours. The straight lines obtained in figure 5.5 have a slope 2k, the rate constant.

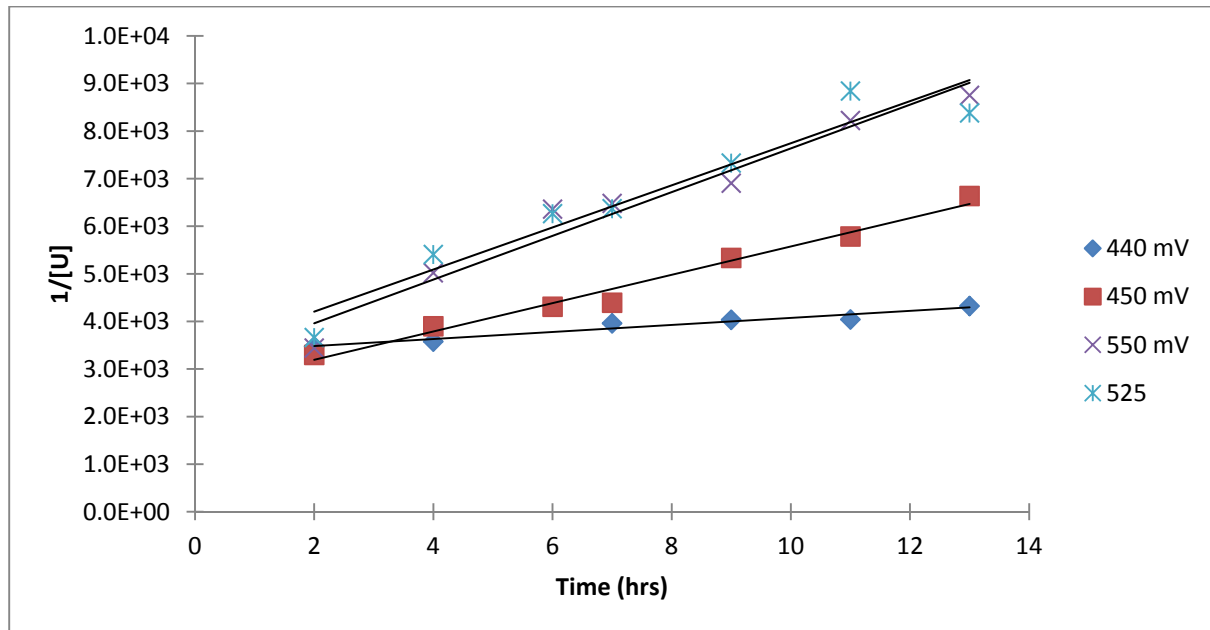


Figure 5. 5: Plot of 1/[U] vs. Time for the tested ORP

The first two hours kinetics was left out of this plot because it is mainly the secondary uranium which does not require oxidation that is believed to leach first. The observed second order kinetics is not in agreement with studies reported by Ram (2013) under the following conditions: Fe(III) : $8.4 \times 10^{-4} - 1.7 \times 10^{-3}$ M, ORP : 420 – 565 mV, H₂SO₄ : 0.15 M. Ram (2013) reported that UO₂ closely followed the first-order kinetics.

The difference in the reaction order reported here and Ram (2013) may be due to the gangue minerals associated with uraninite in this study. Ram (2013) reported that gangue minerals may alter uranium dissolution, the degree of recovery and elevated reactant consumption. He suggested that the foreign ion released may influence the UO₂/UO₂²⁺ dissolution reactions.

Studies done by Rio Tinto’s Technology and Innovation team (T&I) found that run of mine (ROM) material consisted predominantly of quartz, feldspar, hornblende, mica, clay (kaolinite and chlorite), pyroxene (diopside and augite) and carbonate.

The table below shows the rate constants obtained from second order integrated rate law with corresponding ORP values.

Table 5. 5: The rate constant with ORP

ORP (mV)	Rate constant (L mol ⁻¹ h ⁻¹)	R ²
440	37.0	0.94
450	139	0.98
475	168	0.91
500	215	0.93
525	221	0.93
550	231	0.96

Figure 5.6 shows the effect ORP has on uranium dissolution rate. It is a plot of the data shown in table 5.5. It is observed that the increase of ORP results in an increased rate of uranium dissolution, agreeing with the results reported by Ram *et al.*, (2011).

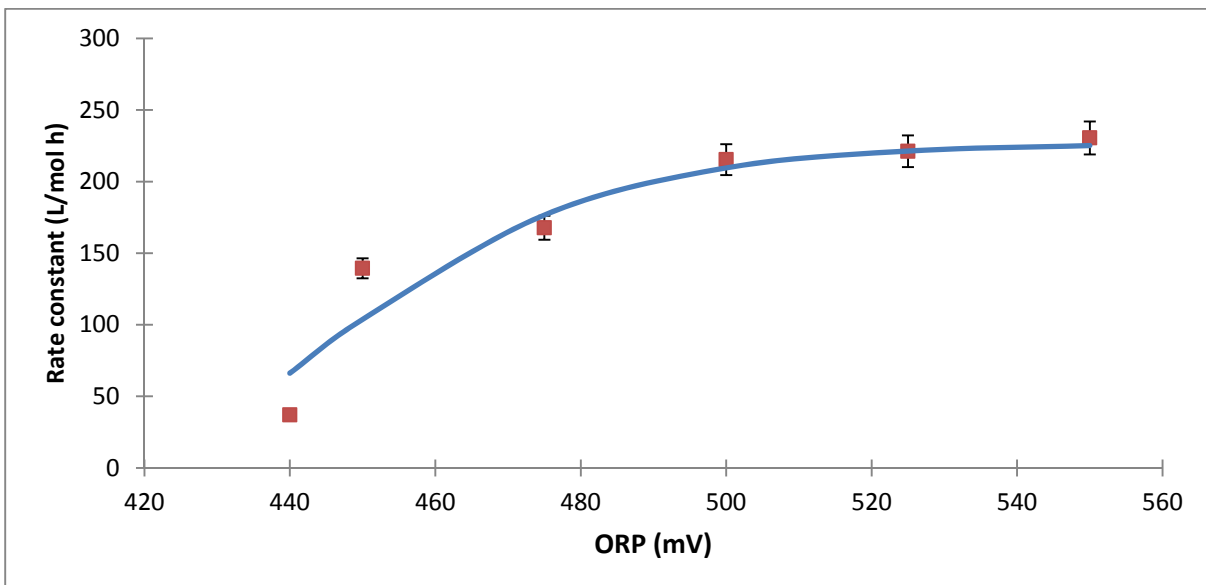


Figure 5. 6: The effect of ORP on dissolution rate of Rössing Uranium ore

The dissolution rate seems to plateau as the ORP exceeds 520 mV. Figure 5.6 illustrates that there is no further benefit gained in operating above 520 mV in terms of the rate of reaction and this finding supports Filippov and Kanevskii (1965) who suggested that maintaining the potential at such a high level is simply a waste of oxidizer. Above 520mV, most of the iron was found to be in ferric state (this is shown in table 5.3). Ferric ion, in the form of ferric sulfate oxidises tetravalent uranium by an electrochemical mechanism in which the concentration of Fe(III) ion adsorbed on the surface determines the rate of reaction (Laxen, 1973).

The Nernst equation (in absence of other electrochemical couples that could affect the potential) equates Fe(III)/Fe(II) ratio to ORP, therefore it can be said that the higher the ORP, the higher the proportion of Fe(III) ion in solution and this is indeed what was found (table 5.3). The correlation between the Fe(III)/Fe(II) ratio and ORP which was established at Rössing Uranium using plant solution (by Rössing Uranium workers) is given by equation 2.15. A good correlation between the measured and modeled ORP using equation 2.15 is shown in the graph below.

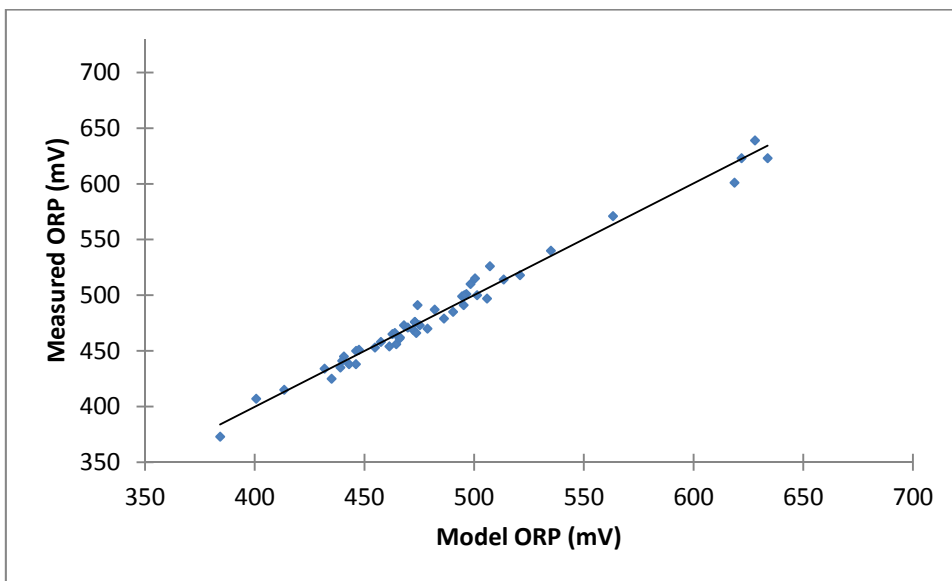


Figure 5. 7: Comparison between modeled and measured ORP

Equation 2.15 is essentially the Nernst equation and it also shows that the increase in Fe(III)/Fe(II) ratio results in increased ORP. This also shows that no other redox couples play a significant role.

5.2.2 Effect of Fe(III) ion on leach kinetics

Total iron concentrations of 0.054, 0.072, 0.081 and 0.090 M were used to understand the effect of Fe(III) ion concentration on uranium leach kinetics. The range considered was based on what could be practical on the processing plant where the downstream processes are taken into account.

These leaches were conducted under the same conditions, only varying the iron concentration. pH and ORP were kept constant at 1.6 and 525 mV respectively. The graph below shows the effect that iron concentration has on the leach kinetics under the above conditions. Figure 5.7 shows that the dissolution rate increased as the iron concentration was increased at constant ORP.

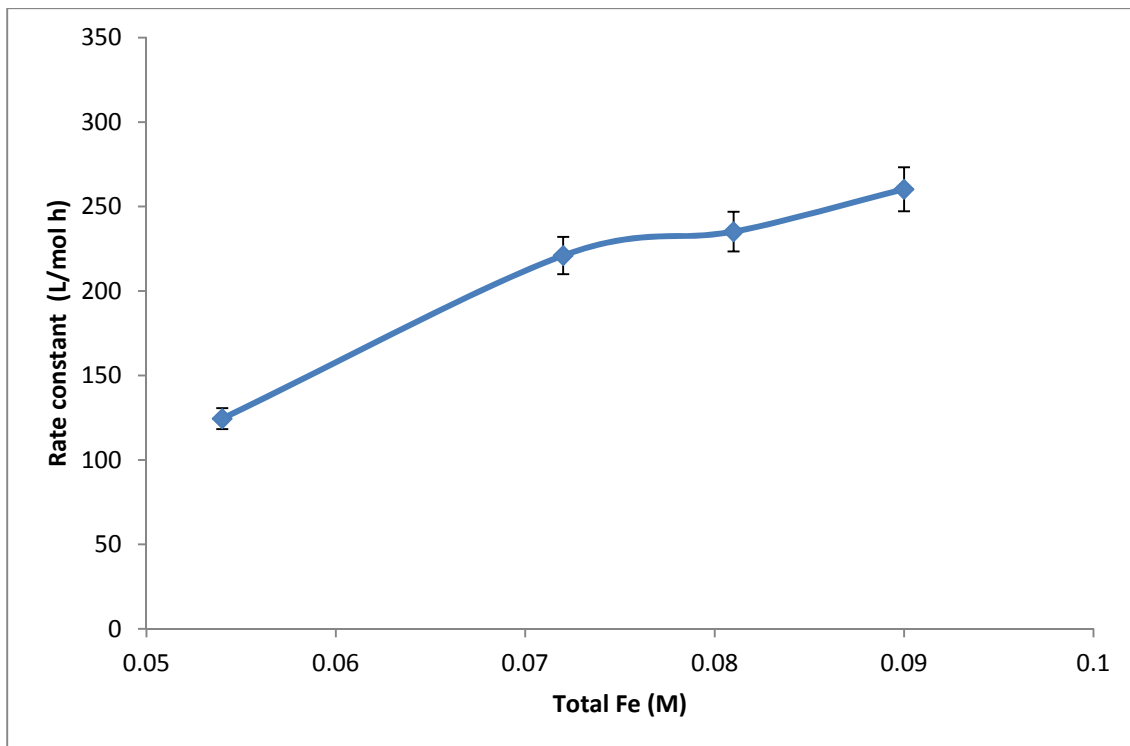


Figure 5. 8: The effect of total iron on the uranium dissolution rate at 525 mV

This result is in agreement with what Dutrizac and MacDonald (1974) reported. Merritt (1971) reported that the increase in the rate of dissolution of uranium indicates a surface chemical reaction in which the concentration of Fe(III) ion adsorbed on the mineral surface determine the rate of the reaction. Since the active Fe(III) ion species adsorb on the uranium surface, Laxen (1973), the amount adsorbed could control the rate of reaction. The amount of Fe(III)

ion adsorbed would be related to the concentration in solution by an adsorption isotherm, therefore the dissolution rate would also be related to the concentration in solution by an adsorption isotherm (Laxen, 1973). If equation 2.30 is considered, it is easy to see that the dissolution rate is dependent on the concentration of uranium. However, this dependence is related to a specific iron concentration as was established by Ram (2011), which means the amount of iron present would determine the dissolution rate. By implication, it can be said that the higher the iron concentration the faster the dissolution rate.

As alluded to earlier, Fe(III)/Fe(II) ratio is intimately associated to ORP. It should be noted that the influence of ORP on the dissolution rate of uranium is dependent on the iron concentration. The graph below shows how the dissolution rate of UO_2 is dependent on iron concentration. Table 5.6 compares the rate constants of different iron concentration at the same ORP. The rate constants were obtained from the second order integrated rate.

Table 5. 6: Rate constant obtained from the second order integrated rate law for different iron concentration at the same ORP

ORP (mV)	Total Fe 0.054 M		Total Fe 0.072 M	
	K (L/mol h)	R ²	K (L/mol h)	R ²
450	139.11	0.93	148.92	0.98
500	153.75	0.96	211.42	0.96
550	165.83	0.92	230.48	0.96

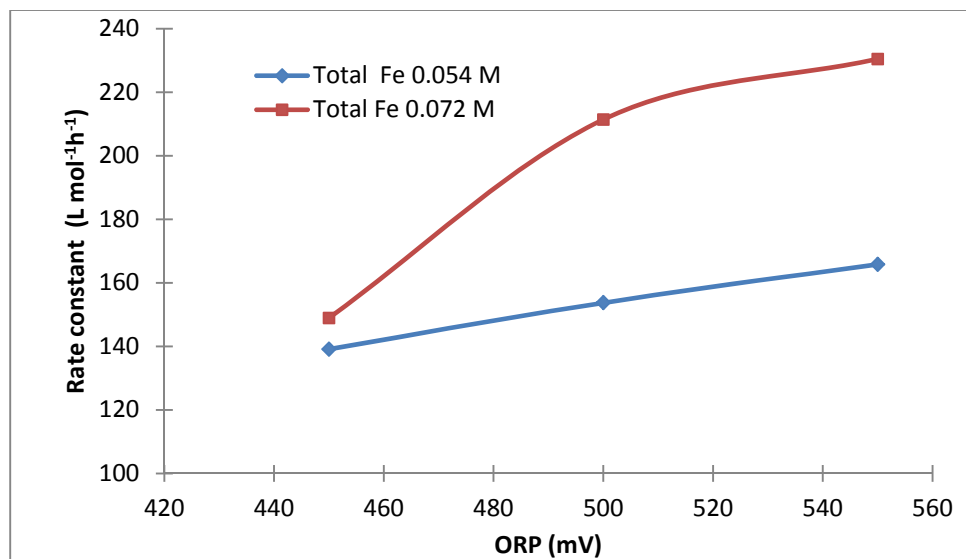


Figure 5. 9: Effect of total iron on the dissolution rate

It can be seen in figure 5.9 that the dissolution rate is different for different iron concentrations at the same ORP agreeing with Ram (2011) who reported that the relationship between the rate of dissolution and [Fe] is not the same in different concentration ranges of Fe even if the ORP ($Fe^{III}:Fe^{II}$ ratio) is identical. The rate is higher for higher iron concentration.

An ORP value may be achieved by any total iron concentration. This can be seen when equation 2.23 (Nernst equation) is taken into account. To illustrate this, let us take 525 mV as an example. At 525 mV, there will be different concentrations of $Fe(III)$ ion in solution, depending on the total iron concentration (see table 5.7). The high total iron concentration would have a higher $Fe(III)$ ion concentration in solution and consequently a higher dissolution rate. Therefore, a combination of high ORP and iron concentration is required to have faster dissolution rates which confirm Fillippov and Kanevskii's (1965) reported findings.

Table 5. 7: Fe (III) concentration at 525 mV for different total iron

Iron concentration	Fe (III) (M)	Fe (II) (M)
0.054 M	0.048	0.007
0.072 M	0.065	0.010

At 550 mV with an iron concentration of 0.054 M, the ferric concentration in the pulp was determined to be equivalent to the ferric concentration at 500mV for a total iron concentration of 0.072 M. Therefore one would expect to see the same extraction achieved at this point and that is what is observed in figure 5.10.

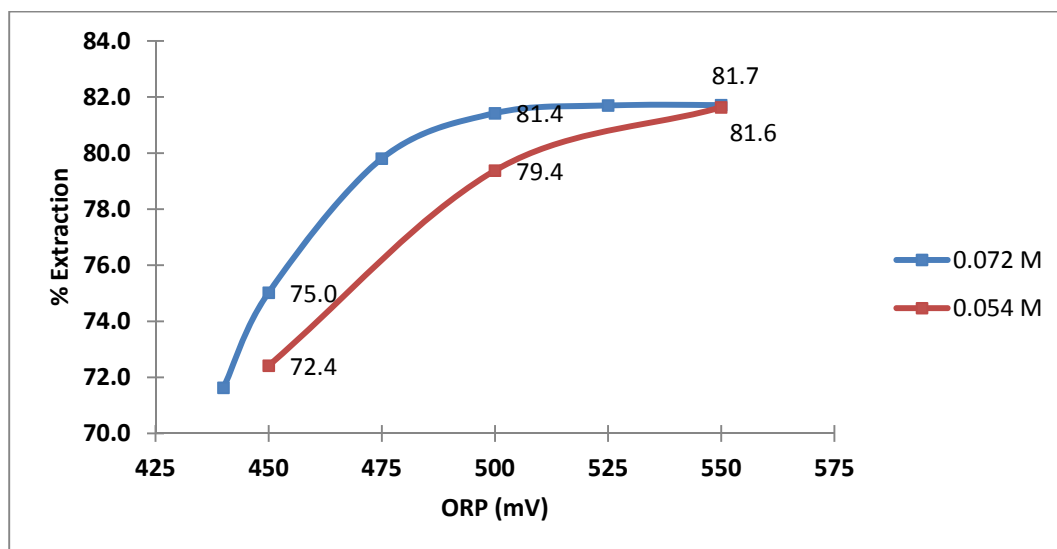


Figure 5. 10: The extraction achieved after 13 hours of leaching at different ORP values

The results obtained in this study show that a higher iron concentration of 0.072 M achieved a higher extraction after 13 hours leach time compared to the lower iron concentration of 0.054 M at each ORP between 450 and 525 mV. This may indicate that ferric concentration has a major part to play in UO_2 dissolution and final extraction.

5.2.3 The effect of pH on uranium dissolution rate

The pH was also varied in order to understand the effects it may have on leach kinetics of the Rössing Uranium ore. The pH values considered in this study were 1.0, 1.2, 1.3, 1.6, and 1.9. ORP and total Fe concentration were kept constant at 525 mV and 0.072 M respectively.

Maintaining the correct free acid concentration is important to ensure that re-precipitation of the uranium does not occur (Bhargava, *et al.*, 2015). So it was necessary to pick the upper bound pH in the area where Fe(III) ion will still be in solution. The results shown in figure 5.11 indicate that pH has an effect on dissolution rate. From the mechanism discussed, it was concluded that the acid is not directly involved in uranium dissolution. The effect shown in the graph below is indirect. H^+ is involved in the re-oxidation of Fe(II) to Fe(III) which is responsible for U^{4+} oxidation to U^{6+} .

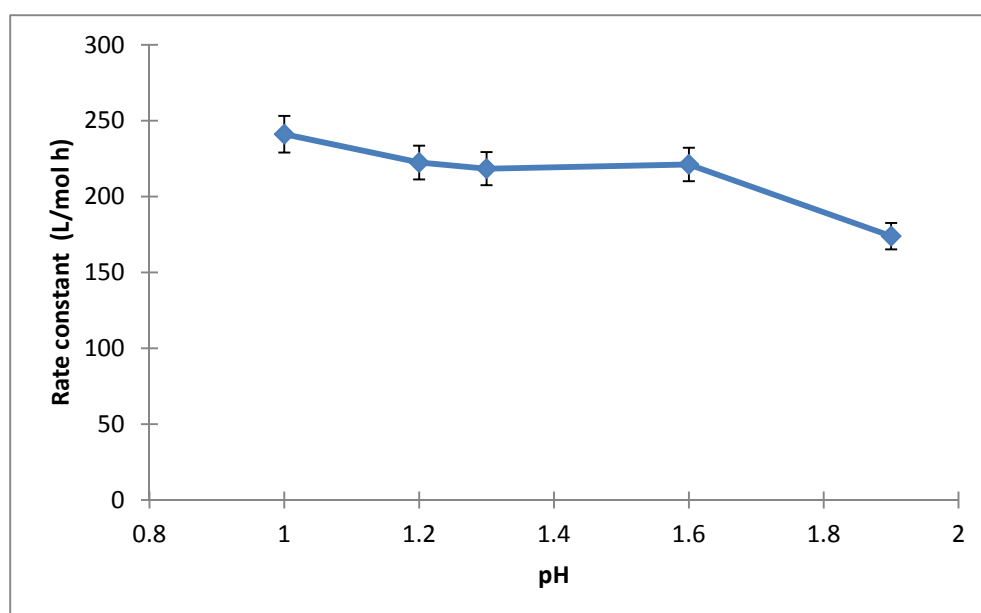


Figure 5. 11: The effect pH has on uranium dissolution rate

Figure 5.11 shows a decrease in the uranium dissolution rate as the pH is increased, supporting the results reported by many researchers (Ibrahim *et al.*, 2013; Eligwe and Torma, 1982). Studies done by Laxen (1973) have shown that the influence the pH has on leach kinetics depends on the ore type. For the ore used in this study, it is clearly observed that the increase in pH results in a decreased dissolution rate albeit that acid is not directly involved in the dissolution reaction.

The pH value at which Fe(III) ion will start to precipitate depends on the Fe(III) ion concentration as well as temperature and ionic strength of the solution. At pH values higher than 2, ferric ion are increasingly bound up in hydrated complexes and therefore contribute less to the redox potential. This would result in a reduced overall dissolution rate (Zachariades and Fraser, 1991). Hydrolysis of Fe(III) ion could therefore be avoided by keeping the pH below 2 at 35°C. Above 130°C ferric iron tends to precipitate fairly rapidly even from solutions of pH as low as 1, forming simple or/and complex basic oxides (Demopoulos, 1985).

Figure 2.9 shows how Fe(III) concentration decreases as the pH is increased. This may explain why the dissolution rate would also decrease as pH increases. The overall extraction also indicates that the increase in pH results in the decrease in overall extraction. Nicol (1981) reported that it is generally accepted that the extraction of uranium is increased by increasing the concentration of acid. This may be because at low pH, concentration H⁺ ion is high which is required in the re-oxidation of ferrous ion to ferric ion and to maintain dissolved uranium in solution.

5.3 Full factorial design

The factors considered were ORP, iron concentration and pH at two levels. The total treatments obtained for three factors at two levels are 8. The minimum (-1) and maximum (+1) levels assigned to the parameters are given in table 5.8. The level selection was based on what is practical in the Rössing Uranium processing plant and also on the previous work done on the plant.

Table 5. 8: List of the process parameters and their levels

Labels	Process parameters	Units	Low level (-1)	High level (+1)
A	ORP	mV	440	525
B	Fe	g/L	3	4
C	pH		1.6	1.9

Other parameters were: pulp density = 70% solids, rpm = 470, retention time = 13 hours

The SigmaXL software package was used to analyse the results obtained from this study. The table below is the coded design matrix generated from the parameter input.

Table 5. 9: Coded design matrix for the three parameters and the response

Standard run order	Actual run order	A	B	C	AB	AC	BC	ABC	Rate constant (L/mol h)	StaDev	Variance
1	1	-1	-1	-1	1	1	1	-1	61.06	2.08	4.34
2	2	1	-1	-1	-1	-1	1	1	121.77	7.76	60.24
3	3	-1	1	-1	-1	1	-1	1	53.26	1.35	1.81
4	4	1	1	-1	1	-1	-1	-1	220.95	7.63	58.16
5	5	-1	-1	1	1	-1	-1	1	39.34	1.62	2.62
6	6	1	-1	1	-1	1	-1	-1	96.58	2.83	8.00
7	7	-1	1	1	-1	-1	1	-1	79.14	2.72	7.41
8	8	1	1	1	1	1	1	1	159.13	5.57	30.98

The findings and discussions are covered in the subheadings below.

5.3.1 The main effect that affect uranium leach kinetics

A main effect can be looked at as the effect of one of the independent variables on the dependent variable while discounting the effects of all other independent variables. The Pareto chart in figure 5.12 shows the significant factors in uranium leach kinetics. The chart shows that the ORP is the most significant factor (within the range of values considered in this experiment) indicating that the extraction is highly dependent on it, followed by the total iron concentration and then interaction between total iron concentration and ORP. All other factors/interactions are statistically significant except Fe x pH interaction.

The dependence of leach kinetics on ORP can be explained by Nicol (1981) who suggested that the uranium leaching reaction is electrochemical in nature. This implies that the right potential should prevail before the leaching of uraninite can take place. The required potential is in this case provided by the Fe(III)/Fe(II) couple. This finding is also supported by Sunder and Shoesmith (1991) who suggested that redox potential is the most important parameter governing the dissolution of UO_2 .

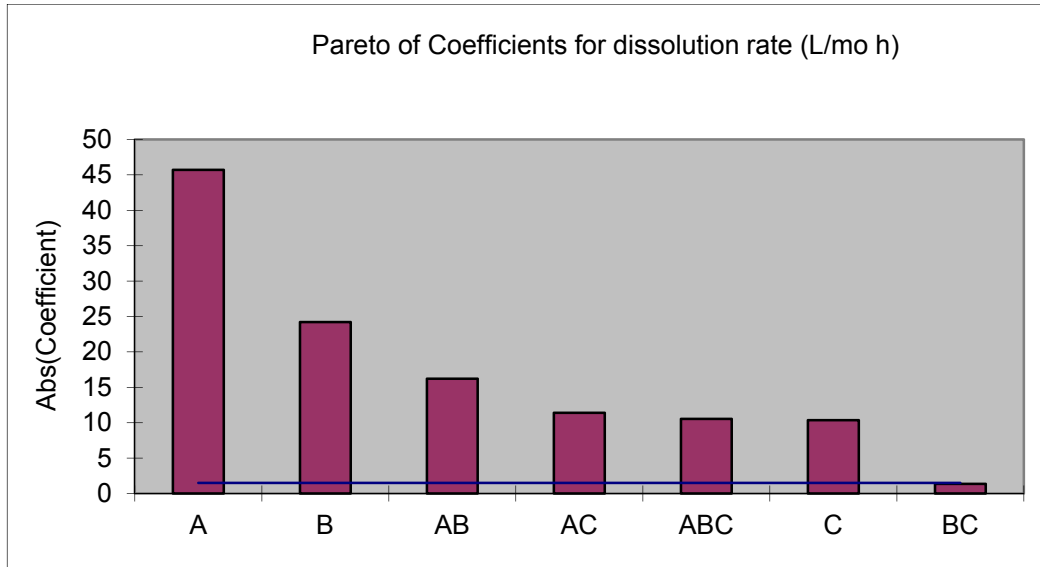


Figure 5. 12: Pareto showing the dominant factors

The total iron is the second in the significant chart as mentioned above. The effect of total iron concentration on leach kinetics has been discussed in 5.2.2 above. The Pareto chart is a great tool to display the relative importance of the main effects and interactions, but it does not tell us about the direction of influence. Figure 5.13 below shows the influence plots of the main effects of ORP, pH and total iron.

It can be observed in figure 5.13(a) that the ORP has the huge impact on uranium leach kinetics followed by total iron concentration whereas pH is observed to have little impact on uranium leach kinetics compared to the other parameters.

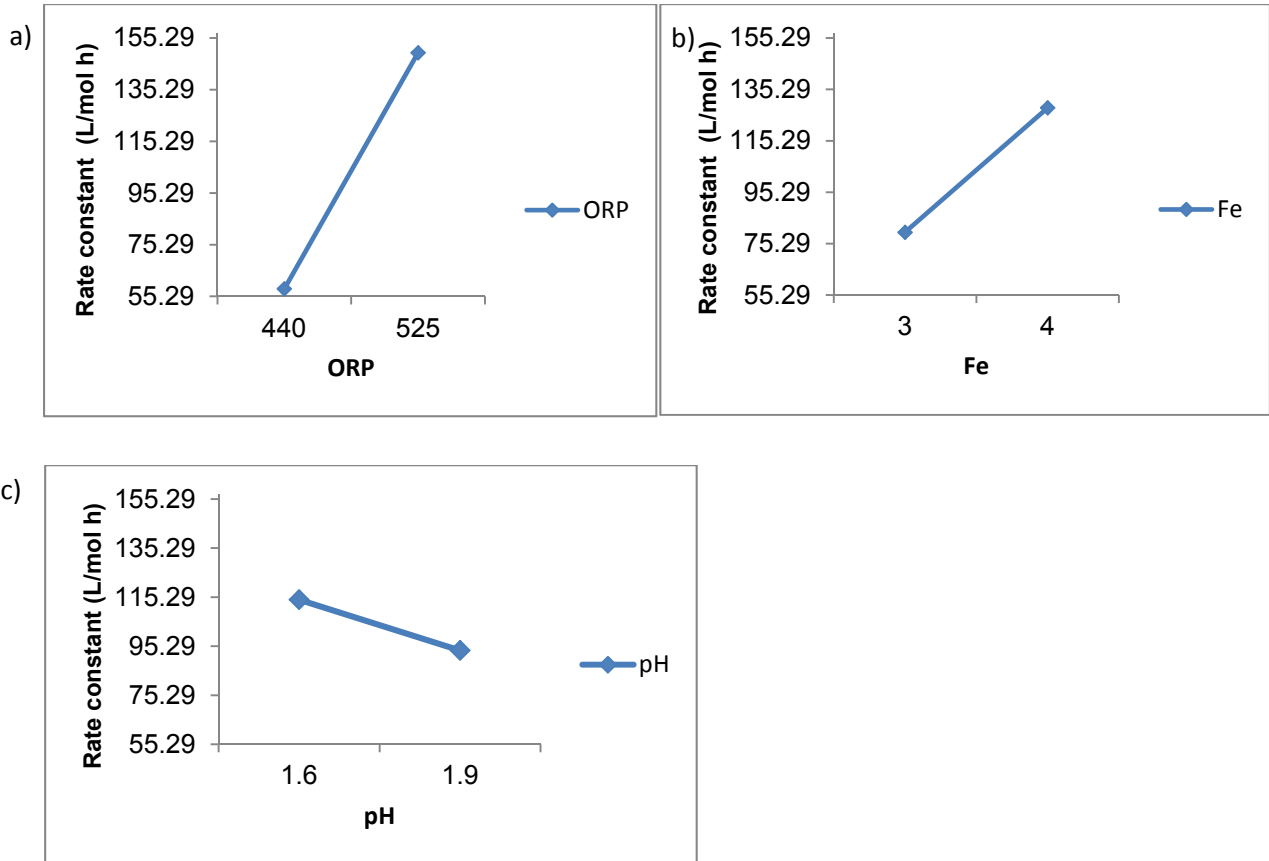


Figure 5. 13: Plots of the main effects; a) the effect of ORP on uranium leach kinetics, b) the effect of Fe on uranium leach kinetics, and c) the effect of pH concentration on uranium leach kinetics.

Figure 5.13(c) shows that an increase in pH has a negative effect on uranium leach rate. the effect of increasing the pH was discussed in 5.2.3 above.

5.3.2 Effect of factors' interaction on uranium leach kinetics

In figure 5.14, one can observe an interaction between pH and ORP. The interaction clearly shows that as ORP increases, the rate increases for both pH values. The lower pH attains a higher rate compared to the higher pH value. This shows that the pH has an effect on the rate although it is indirect.

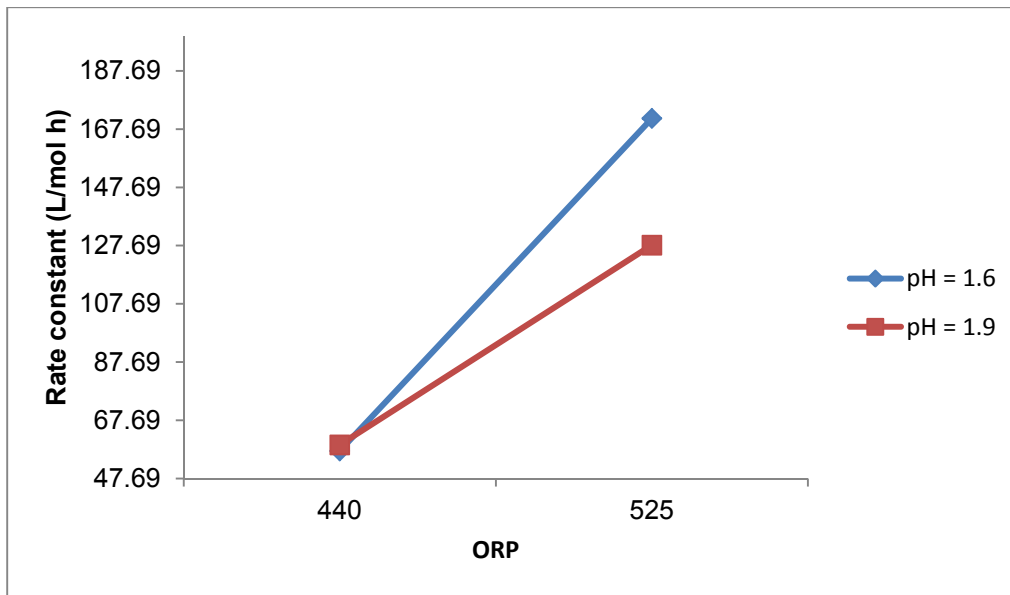


Figure 5. 14: The interaction between ORP and pH

In figure 5.15, the the interaction between ORP and total iron can be observed. As the ORP increases, the leach rate of uranium increases in both iron concentrations. Also notice that the interaction between ORP and iron concentration shows that the higher the iron concentration, the faster the leach rate as ORP increases.

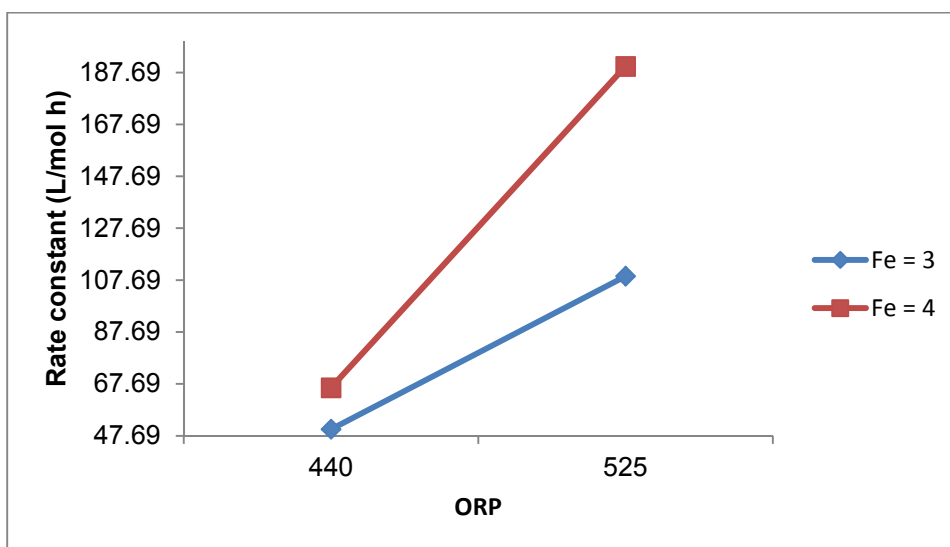


Figure 5. 15: The interaction between ORP and [Fe]

Ram et al., (2011) observed that Fe(III), Fe(II) and solution ORP are very closely related, with solution ORP relying on Fe(III)/Fe(II) ratio. As such the influence that Fe(III) ion, Fe(II) ion and ORP have on the rate of UO_2 dissolution cannot be isolated as changing either Fe(III) ion or

Fe(II) ion concentrations will also lead to a change in solution ORP. However, this is only true for Fe(II) ion if the concentration of Fe(III) ion is not too high as suggested by Nicol and Needes (1975). The rates at lower ORP are close to one another for both total Fe concentrations, this was shown by Ram (2011) that the rate is less dependent on total iron at lower ORP values.

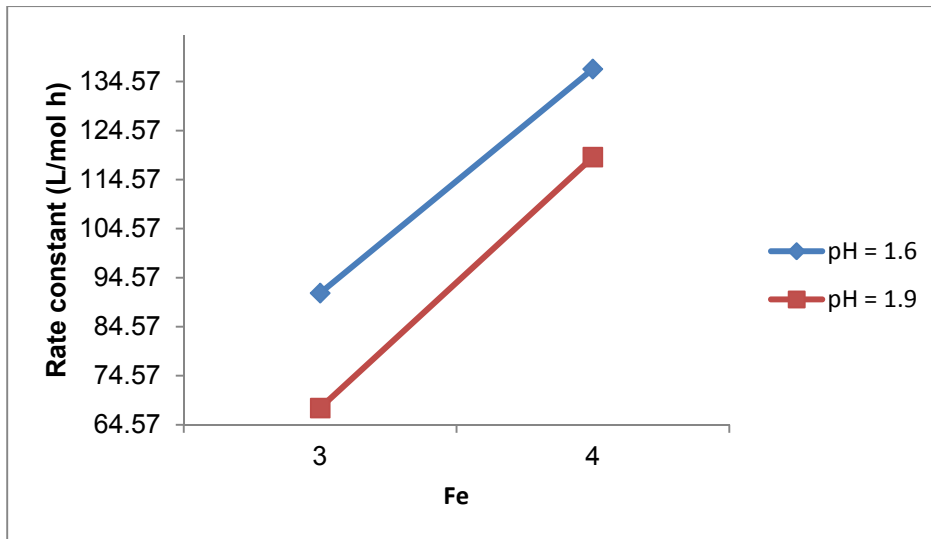


Figure 5. 16: The interaction between total Fe and pH

There is very minimal interaction between total Fe and pH. As the total Fe is increased, the rate increases accordingly for both pH values. This indicates that interaction between pH and total Fe is nominal.

5.4 Leach kinetics model equations

The kinetic data obtained were modelled using a regression method, and a curve fitting approach. Two models were generated from these two approaches. These types of models give a single response based on any change made in the parameters. In order to model the leach kinetics using this approach, it is necessary to determine the rate constant K. The rate constant will then inform to what extent a change in a certain parameter will affect the leach rate. The applicability of the models is discussed below.

5.4.1 Multiple regression model

Multiple Regression can be used to analyse the relationship between one dependent variable such as uranium leach rate and multiple variables such as in this case, ORP, Fe concentration and pH. The empirical equation that is generated is of the form:

$$Y = b_0 + b_1 * X_1 + b_2 * X_2 + \dots + b_n * X_n \quad (5.3)$$

Where Y is the response or rate constant, b_i represents the coefficients and constants terms generated by the least square method and X_i are the input variables. The model should consist of only the variables that have an effect on the response. The three parameters under consideration were all found to be significant in 5.3.1.

The model obtained from the kinetics data is:

$$\text{Rate constant} = ((-463.68) + (1.08)ORP + (48.43)Fe + (-69.03)pH) + 4 \quad (5.4)$$

The interaction between ORP and total iron is significant and one should expect to see it in the question 5.4. However, it is not included in the model because there is no 'physical value' that one can input in the model like the other parameters.

5.4.2 Exponential empirical model

Another way to model kinetic data is by fitting equations to the curves generated from the kinetic data. Software packages that can be used to fit equations to the curves generated from experimental data are available. The package used in this study to generate the model is CurveExpert Professional 2.0.2. This software produces possible models arranged according to the increasing coefficient of determination usually denoted by R^2 . The closer R^2 is to 1, the better the model would fit the experimental data. The model chosen for this data is

$$\text{Rate constant} = \frac{a}{(1 + e^{(b-cx)})^{\frac{1}{d}}} \quad (5.5)$$

Where

$$\begin{aligned} a &= 454.09 \\ b &= 16.02 \\ c &= 0.046 \\ d &= 0.014 \end{aligned}$$

It should be noted that this model has no theoretical basis; it is just a mathematical expression that fits the experimental data well enough.

5.4.3 Evaluation of the kinetic models

The two kinetic models were evaluated on how well they would fit experimental data. Figure 5.17 shows how the multiple regression model predicted rate constants compared to the rate constants determined from experimental data.

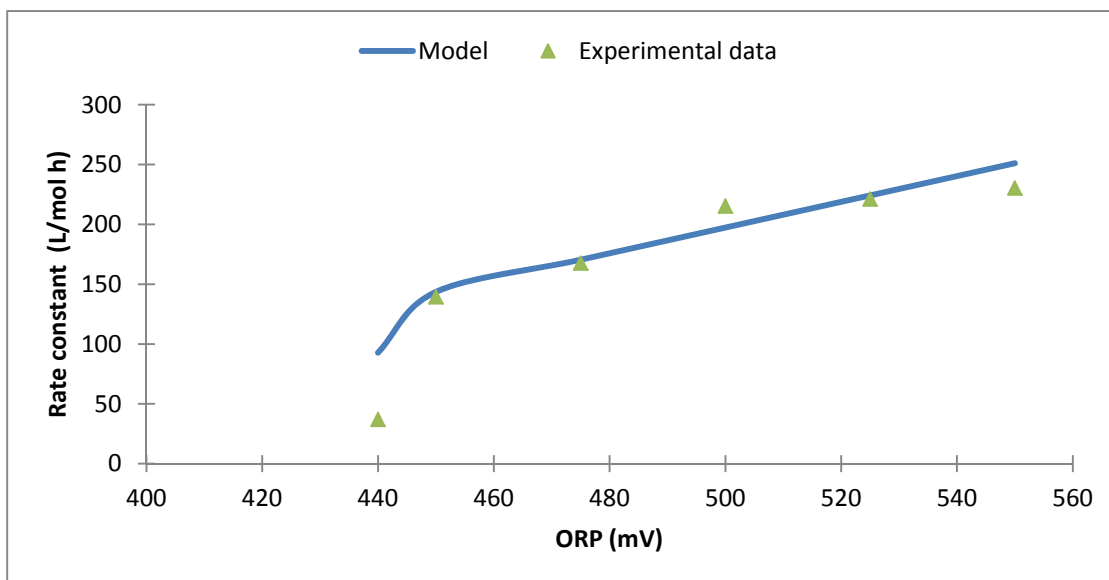


Figure 5. 17: Comparison between the multiple regression model and experimental data

Figure 5.17 shows that the model predicts that the increase in ORP will result in increased leaching rate. The x-axis can be any one of the three parameters. The model would still predict the rate accurately. The model was put into an Excel spread sheet to come up with the interface shown in figure 5.18. For the use on the plant, the setup shown below could be used to input parameters to get the predicted leach rate.

Parameter		Rate constant (L/mol h)
ORP (mV)	525	
Fe (g/L)	4	197.3
pH	1.6	

Figure 5. 18: The model interface

The model generated in this work can test different combinations (as shown in figure 5.18) of parameters in order to investigate their influence on the leach rate and thus find the optimal conditions, within the limits of the chosen parameters. The limits within which the model can operate can be programmed or a simple logic function in Excel can be devised to limit the input values to the required range. The model has been tested on the values considered in this test work and was able to predict the rate constants.

The other model considered in this study is the exponential empirical model, equation 5.5. As indicated above, this model was generated by curve fitting. It can only take into account one variable as an input to predict the leach rate. The other parameters should be kept constant. This is one of the differences between the multiple regression models and this kind of model. Figure 5.19 shows how the model fits the experimental data.

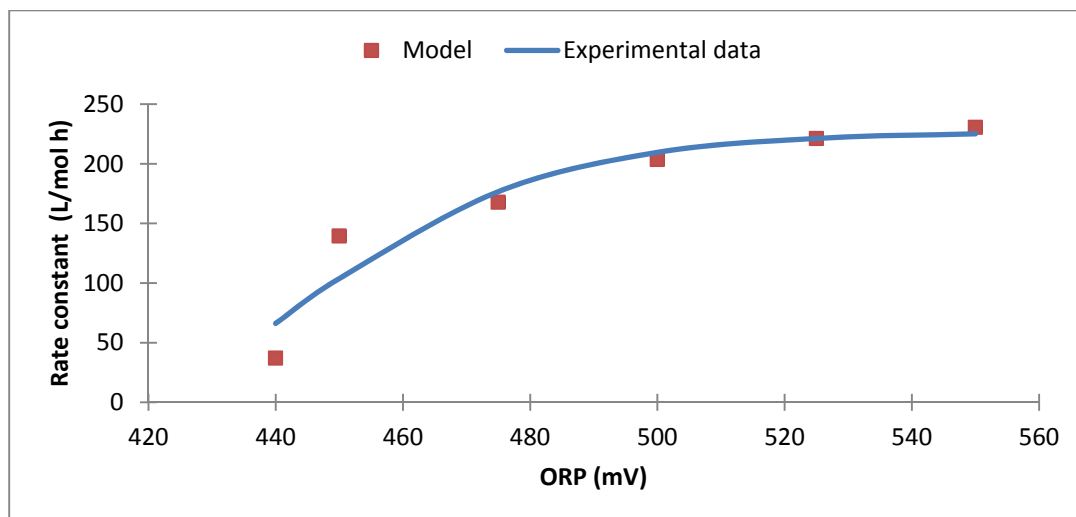


Figure 5. 19: Comparison between the exponential empirical model and experimental data

The exponential empirical model seems to fit the data better than the multiple regression model. It also shows that the increase in ORP will result in increased leach rate. Though it fits the experimental data better than the former, it does not offer the same flexibility as it can only predict the effect of one parameter at a time. This is the reason why one would prefer to work with the multiple regression model which can cater for manipulation of more than one parameter at a time.

The models used can all predict the leach rate satisfactorily, but they do not take into account other physical factors that may affect the rate, such as the ore type or the mixing in the leach vessels. The error in the prediction of the model may include these physical factors. This means the models should be used with this limitation in mind.

Chapter 6: Conclusion and Recommendations

6.1 Conclusion

The study has provided an insight into understanding the leach kinetics of Rössing Uranium ore in terms of the influence that parameters such as the oxidation–reduction potential (ORP), the total iron concentration and pH have on leaching. The kinetics data obtained were used to build models that can be applied to predict the leach dissolution rate of Rössing Uranium ore.

The study found that an increase in ORP resulted in an increased dissolution rate of uranium because a high ORP indicates a high concentration of Fe(III) ion which is required to oxidise uraninite. The dissolution rate was found to be directly proportional to the increase in total iron.

The influence of ORP was found to depend on the iron concentration in the slurry. This is because a high concentration of iron would result in a higher Fe(III) ion concentration at high ORP values. The pH has an indirect influence on dissolution rate. An increase in the pH resulted in a decrease of the dissolution rate of uranium.

The dissolution of uranium was found to follow the second order. Two models were generated from the kinetic data using multiple regression and curve fitting approaches. The multiple regression model is preferred over the other mainly because it can accommodate the change in all three variables at once and has showed a good fit with the experimental data.

6.2 Recommendations

A future study should look at:

- The effect the complexing ion such as SO_4^{2-} and NO_3^- typically found in Rössing Uranium solutions have on uranium dissolution. Studies done by Ram (2013) have shown that these ion would affect the rate of leaching uranium.
- The same study using other oxidants such as hydrogen peroxide, sodium chlorate and oxygen and compare the dissolution rates using these oxidants. Added to this is to quantify the benefits Rössing Uranium could gain from elevated temperature leaching.
- The link between mineralogy and leaching rate of uranium bearing ores.

References

- Ajuria, S., Joe, E. G., Murthy, T. K. S., Peterson, H. D., Seidel, D. C. & Stsrgarsek, A. (1990). Manual on Laboratory Testing for Uranium ore processing. Technical Reports Series No. 313. Vienna, International Atomic Energy Agency.
- Bhappu, R. B., Johnson, P. H., Brierley, J. A., & Reynolds, D. H. (1969). Theoretical and practical studies on dump leaching. *AIME Trans*, 244, 307-320.
- Bhargava, S. K., Ram, R., Pownceby, M., Grocott, S., Ring, B., Tardio, J., & Jones, L. (2015). A review of acid leaching of uraninite. *Hydrometallurgy*, 151, 10-24.
- Burkin, A. R. (2001). *Chemical hydrometallurgy: Theory and principles* (Vol. 1). World Scientific.
- Casas, J. M., Crisóstomo, G., & Cifuentes, L. (2005). Speciation of the Fe (II)–Fe (III)–H₂SO₄–H₂O system at 25 and 50° C. *Hydrometallurgy*, 80(4), 254-264.
- Crundwell, F. K. (1995). Progress in the mathematical modelling of leaching reactors. *Hydrometallurgy*, 39(1), 321-335.
- Crundwell, F. K. (2013). The dissolution and leaching of minerals: mechanisms, myths and misunderstandings. *Hydrometallurgy*, 139, 132-148.
- Demopoulos, G. P. (1985). Acid pressure leaching of a sulphidic uranium ore with emphasis on radium extraction. *Hydrometallurgy*, 15(2), 219-242.
- Dutrizac, J. E., & MacDonald, R. J. C. (1974). *Ferric ion as a leaching medium*. Dept. of Energy, Mines, and Resources, Ottawa.
- Eligwe C.A, Torma A.E., & Devries, F.W. (1982). Leaching of uranium ores with the H₂O₂--Na₂SO₄--H₂SO₄ system. *Hydrometallurgy*, 9(1), 83 --95.
- Filippov, A. P., & Kanevskii, E. A. (1965). Oxidation-reduction potentials and the degree of uranium leaching in sulphuric acid solutions. *Journal of Nuclear Energy. Parts A/B. Reactor Science and Technology*, 19(7), 575-580.
- Ford, M. A. (1993). Uranium in South Africa. *Journal of The South African Institute of Mining and Metallurgy*, 93(2), 37-58.

Gogoleva, E. M. (2012). The leaching kinetics of brannerite ore in sulfate solutions with iron (III). *Journal of Radioanalytical and Nuclear Chemistry*, 293(1), 185-191.

Gupta, C. K., & Mukherjee, T. K. (1990). *Hydrometallurgy in extraction processes* (Vol. 2). CRC press.

Hayes, P. C. (2003). *Process principles in minerals and materials production*.

Hennig, C., Schmeide, K., Brendler, V., Moll, H., Tsushima, S., & Scheinost, A. C. (2007). The Structure of Uranyl Sulfate in Aqueous Solution- Monodentate Versus Bidentate Coordination. *X-Ray Absorption Fine Structure--XAFS 13*, 882, 262-264.

Ho, E. M., & Quan, C. H. (2007). Iron (II) oxidation by SO₂/O₂ for use in uranium leaching. *Hydrometallurgy*, 85(2), 183-192.

Hyams, D. G. (2010). CurveExpert software, <http://www.curveexpert.net>.

Ibrahim, M. E., Lasheen, T. A., Hassib, H. B., & Helal, A. S. (2013). Oxidative leaching kinetics of U (IV) deposit under acidic oxidizing conditions. *Journal of Environmental Chemical Engineering*, 1(4), 1194-1198.

International Atomic Energy Agency. (1993). *Uranium Extraction Technology*. Technical Reports Series 359. Vienna.

International Atomic Energy Agency. (2001). *Analysis of Uranium Supply to 2050*. IAEA-SM-362/2. Vienna.

James, H. E. (1976). *Recent trends in research and development work on the processing of uranium ore in South Africa* (No. PEL--253). Atomic Energy Board.

Krouwer, J. S. (2002). Setting performance goals and evaluating total analytical error for diagnostic assays. *Clinical Chemistry*, 48(6), 919-927.

Laxen, P. A. (1973). *Fundamental study of the dissolution in acid solutions of uranium minerals from South African ores* (No. NIM--1550). National Inst. for Metallurgy, Johannesburg (South Africa).

Levenspiel, O. (1999). *Chemical reaction engineering 3rd edition*. New York: John Wiley & Sons.

Lottering, M. J., Lorenzen, L., Phala, N. S., Smit, J. T., & Schalkwyk, G. A. C. (2008). Mineralogy and uranium leaching response of low grade South African ores. *Minerals Engineering*, 21(1), 16-22.

Lunt, D., Boshoff, P., Boylett, M., & El-Ansary, Z. (2007). Uranium extraction: the key process drivers. *Journal - South African Institute of Mining and Metallurgy*, 107(7), 419.

Luht, J.L.M. (1998). Anodic dissolution of uranium dioxide in simple electrolyte solutions and simulated ground waters, A thesis submitted for the degree of Master of Science, University of Manitoba, Winnipeg, MB.

Merritt, R. (1971). *The Extractive Metallurgy of Uranium*, Colorado School of Mines Research Institute. Colorado: Res. Inst.

Milivojevic, M., Stopic, S., Friedrich, B., Stojanovic, B., & Drndarevic, D. (2012). Computer modeling of high-pressure leaching process of nickel laterite by design of experiments and neural networks. *International Journal of Minerals, Metallurgy, and Materials*, 19(7), 584-594.

Misra, K. C. (2000). *Understanding Mineral Deposits*. Dordrecht: Kluwer Academic Publishers.

Newton, W. (1975). *The Kinetics of the Oxidation-Reduction Reactions of Uranium, Neptunium, Plutonium, and Americium in Solutions*.

Nicol M.J and Needes C.S.R. (1975). Electrochemical model for the leaching of uranium dioxide, acid media. *Leaching and Reduction in Hydrometallurgy*, 1 - 11.

Nicol, M. (1981). Uranium ore processing: *The chemistry of uranium leaching*. Vacation School. Johannesburg: National Institute of Metallurgy .

Nirdosh, I. (1985). Ferric nitrate leaching of uranium and radium from uranium ores. *Hydrometallurgy*, 15(1), 63-76.

Othusitse, N., & Muzenda, E. (2015). Predictive Models of Leaching Processes: A Critical Review. In 7th International Conference on Latest Trends in Engineering & Technology (ICLTET'2015), Irene, Pretoria (South Africa).

Ram, R., Charalambous, F., Tardio, J., & Bhargava, S. (2011). An investigation on the effects of Fe (Fe III, Fe II) and oxidation reduction potential on the dissolution of synthetic uraninite (UO₂). *Hydrometallurgy*, 109(1), 125-130.

Ram, R. (2013). 'Investigation on the dissolution of synthetic and natural uraninite', A thesis submitted for the degree of Doctor of Philosophy, School of Applied Science, Applied Science, RMIT University, pages 80 – 94, 100 – 158.

Ram, R., Charalambous, F., McMaster, S., Tardio, J., & Bhargava, S. (2013). An investigation on the effects of several anions on the dissolution of synthetic uraninite (UO₂). *Hydrometallurgy*, 136, 93-104.

Ring, E & Ho, B. (2007). Oxidants for Uranium Leaching. *ALTA uranium conference*. Perth: ALTA, 2007.

Ring, R. J. (1980). Ferric sulphate leaching of some Australian uranium ores. *Hydrometallurgy*, 6(1), 89-101.

Rössing, U. (2012). *Homogenisation of bulk samples*. Unpublished internal report., Rössing Uranium Ltd. Swakopmund.

Ryan, E. (2011). *Mineralogy of Rössing bulk control, feed and discharge samples*. Unpublished internal report., Rössing Uranium Ltd. Swakopmund..

Schreuder, H and Roesener CP. (1992). *Uranium*. Windhoek: Geological Survey of Namibia.

SigmaXL. (2014). SigmaXL® Version 7.0 Workbook. In SigmaXL, *SigmaXL® Version 7.0 Workbook*. SigmaXL.

Sillilo, B. (2012). *Determination of iron content in the ore by leaching*. Unpublished internal report., Rössing Uranium Ltd. Swakopmund.

Spitsyn, V. I., Nesmeyanova, G. M., & Vikulov, A. I. (1965). Some features of the process of uranium oxidation by trivalent iron ion. *Journal of Nuclear Energy. Parts A/B. Reactor Science and Technology*, 19(9), 729-735.

Sunder, S and Shoesmith D.W. (1991). *The chemistry of UO₂ fuel dissolution*. Atomic Energy of Canada.

Szubert, A., Łupiński, M., & Sadowski, Z. (2006). Application of shrinking core model to bioleaching of black shale particles. *Physicochemical Problems of Mineral Processing*, 40, 211-225.

Tamrakar, P. K., Prajapati, D., & Sarangi, A. K. (2010). Study of leaching characteristics on low grade uranium ore of Bagjata mine. In *Proceedings of the XI International Seminar on Mineral Processing Technology (MPT-2010)* (Vol. 1, No. Section 8, pp. 666-672). Allied Publishers, New Delhi.

Vernon, P. (1981). Uranium ore processing: *Extraction of Uranium at Rossing Uranium Limited*. Vacation School. Johannesburg: National Institute of Metallurgy .

Wolf, R. (2005, March). What is ICP - MS? Research Chemist, USGS/CR/CICT.

World Energy Council. (2013). *World Energy Resources*. London: World Energy Council.

Zachariades, J. C., & Fraser, D. M. (1991). Experimental and modelling studies of the kinetics in the leaching of pyrolusite. *Journal of the South African Institute of Mining and Metallurgy(South Africa)*, 91(8), 277-285.

Appendices

Appendix A

Determination of percentage relative standard deviation for the leach tests

Overall sampling error						
Sample time (hrs)	Assay 1	Assay 2	Assay 3	Average	% extraction	
2.5	0.0258	0.0248	0.0268	0.0258	91.308	
5	0.0263	0.025	0.0273	0.0262	91.173	
7	0.0258	0.0252	0.0247	0.0252	91.499	
9	0.0253	0.0246	0.0237	0.0245	91.735	
11	0.0277	0.0268	0.0267	0.0271	90.882	
13	0.026	0.0274	0.0259	0.0264	91.095	
				Mean	0.0259	91.2821
				STDV	0.0009	0.3034
				%RSD	3.4800	0.3324
				95% CI	0.0018	0.6068

$\%RSD = \text{SDTV}/\text{mean} \times 100$

$95\% \text{ CI} = 2\text{SDTV}$

Determination of analytical error

Test	Standard deviation in repeat assays	%RSD	# of repeats per sample	Standard Error	Relative Standard Error (%)
Triplicate assay	0.19	0.21	3	0.11	0.12
5 repeat assay	0.18	0.20	5	0.08	0.09

Determination of sub- sampling error from the vessel

Sample	Mean (ext %)	STDEV (ext %)	%RSD	95% CI
In-situ	92.2	0.87	0.94	1.74

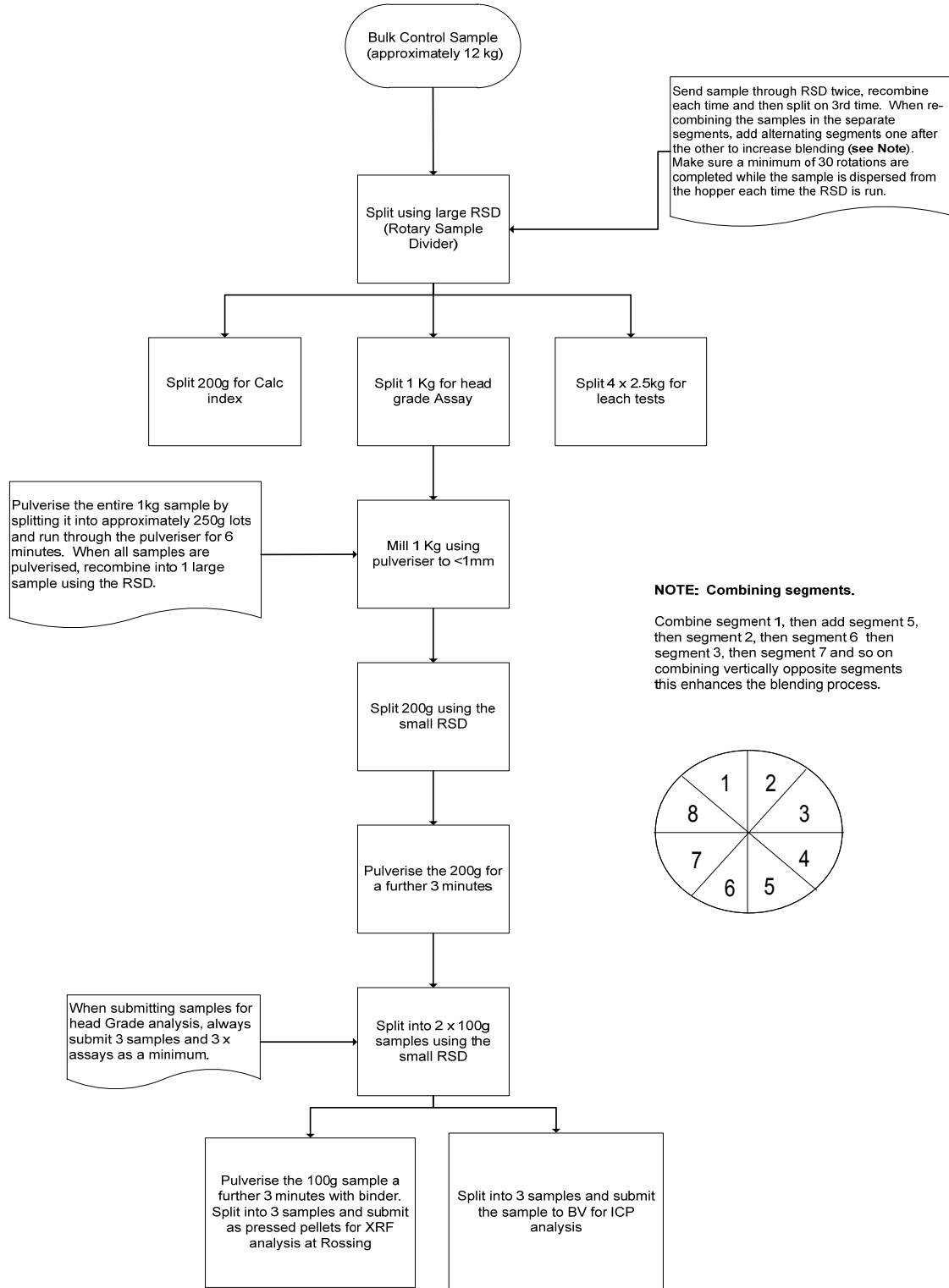
Determination of sub-sampling error from the final leach residue

Test	Mean (ext %)	STDEV (ext %)	%RSD	95% CI
Two leach	92.6	0.33	0.35	0.65



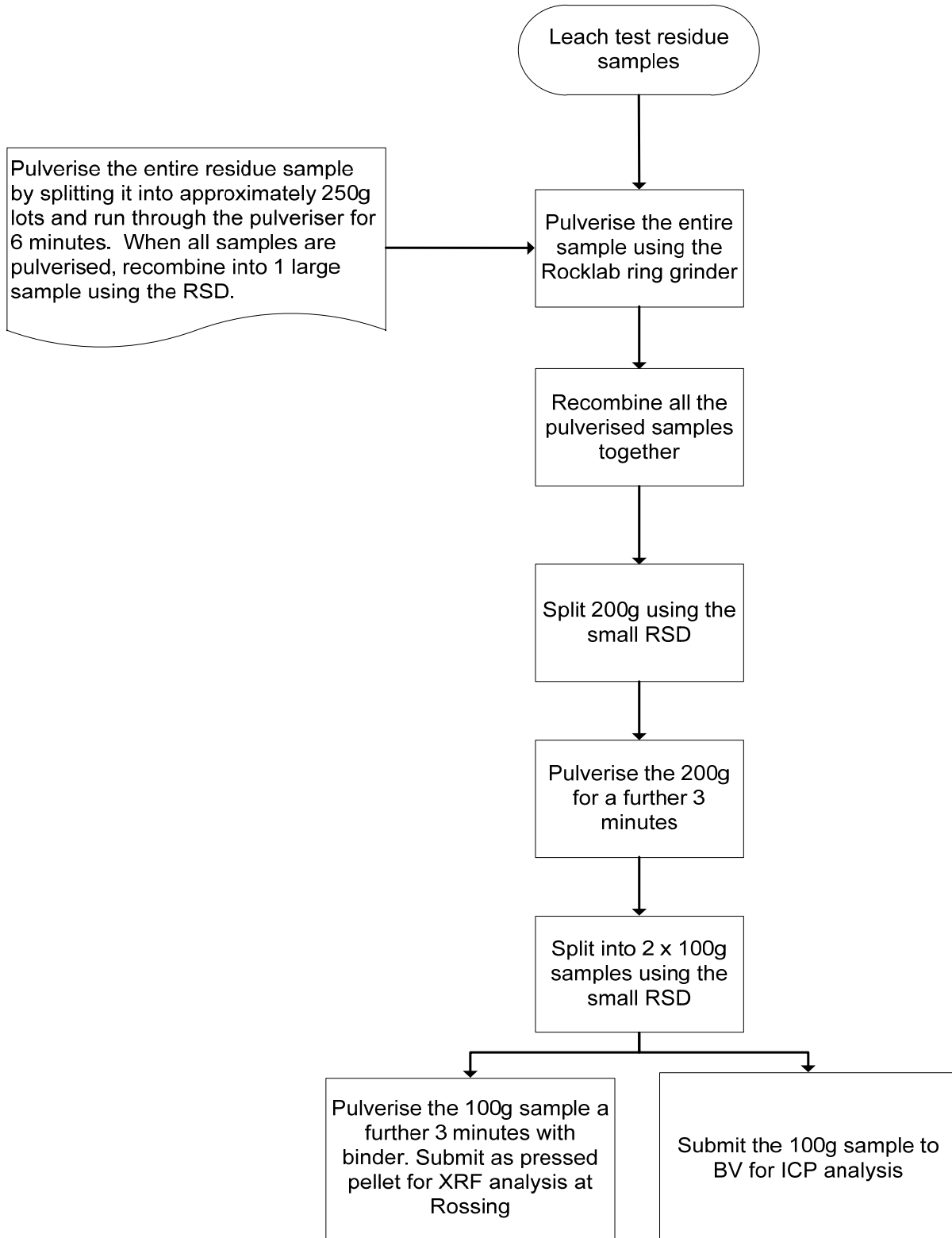
Appendix B

Bulk Control Sample Preparation



Appendix C

Preparation of residue sample for analysis



Appendix D

Determination of ferric/ferrous in plant solutions

1. Determination of ferrous iron (Fe^{2+}) in plant solution

Procedure

1. Pipette 10ml sample into a conical flask (use Pipette Filler).
2. Add 5ml spekker acid to conical flask using jigger.
3. Add 2-3 drops sodium diphenylamine sulphonate indicator.
4. Titrate with standard potassium dichromate solution until the first purple colour.
5. Note titre on worksheet.

2. Determination of ferric iron (Fe^{3+}) and free sulphuric acid in plant solutions

Procedure

1. Pipette 10ml sample into a clean 150ml beaker (use Pipette Filler).
2. Add approximately 1 gram potassium iodide.
3. Allow standing for at least 3 minutes.
4. Titrate the liberated iodine with standard sodium thiosulphate solution to a faint yellow colour.
5. Add a few drops starch solution.
6. Continue the titration until the blue colour just disappears.
7. Add 3ml more of the thiosulphate to the sample.
8. Add three drops of mixed indicator.
9. Titrate with sodium carbonate until the first green colour.

Appendix E

Uranium containing minerals

Mineral	Formula
Betafite	$(Ca, U)_2(Ti, Nb, Ta)_2O_6(OH)$
Uranophane	$Ca(UO_2)_2SiO_3(OH)_2 \cdot 5(H_2O)$
Uraninite	UO_2
Biotite	$K(Mg, Fe^{2+})_3[AlSi_3O_{10}(OH, F)_2]$
Brannerite	$(U^{4+}, Ca)(Ti, Fe^{3+})_2O_6$
Monazite	$(Ce, La, Th, Nd, Y)PO_4$



Appendix F

Three-Factor, Two-Level, 8-Run, Full-Factorial Design of Experiments

Three-Factor, Two-Level, 8-Run, Full-Factorial Design of Experiments

Title: Mr
Date: 2016/07/01
Name of Experimenter: B Sililo
Response: Dissolution rate
Goal:

Factor	Factor Name	Low	High
A	ORP	440	525
B	Fe	3	4
C	pH	1.6	1.9

Predicted Output for Y:

Factor Name	Enter Actual Factor Setting - uncoded	Factor setting coded	Y-hat:	S-hat:
	0	-11.353	9188.6	-192.8
	0	-7		
	0	-11.667		

Experimental Worksheet:

Outer Array or Response Replicates:

StandardRun Order	ActualRun Order	ORP	Fe	pH	Rate (L/mol h)	Average (rate (L/mol h))	StdDev				
1		440	3	1.6	63.315	58.45	62.04	62.205	59.275	61.057	2.083
2		525	3	1.6	127.94	111.9	117	130.85	121.18	121.77	7.7618
3		440	4	1.6	54.47	53.415	51.705	54.645	52.07	53.261	1.3454
4		525	4	1.6	216.94	221.71	231.71	223.21	211.2	220.95	7.6264
5		440	3	1.9	39.772	41.452	38.762	37.021	39.716	39.344	1.6202
6		525	3	1.9	96.465	96.43	93.69	101.22	95.12	96.584	2.8285
7		440	4	1.9	79.815	75.94	77.17	82.965	79.81	79.14	2.7229
8		525	4	1.9	151.51	163.48	154.88	163.36	162.45	159.13	5.5662